Topological excitations in nano-scale ferroelectrics

Domains, vortices, skyrmions…

Igor Lukyanchuk

University of Picardie, France

** Supported by H2020-ITN-NOTEDEV, H2020-RISE-ENGIMA*

What is Ferroelectric ?

Crystal with di-polar moment P

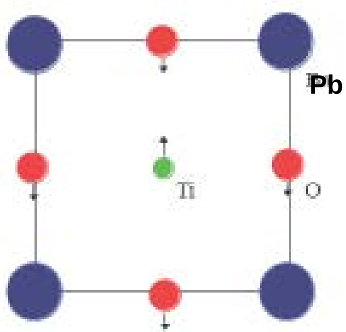

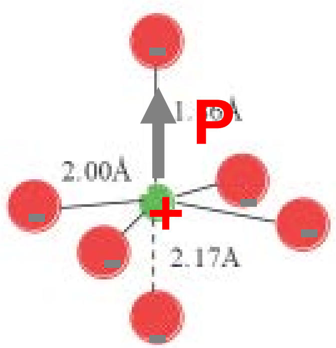

Perovskite: PbTiO3

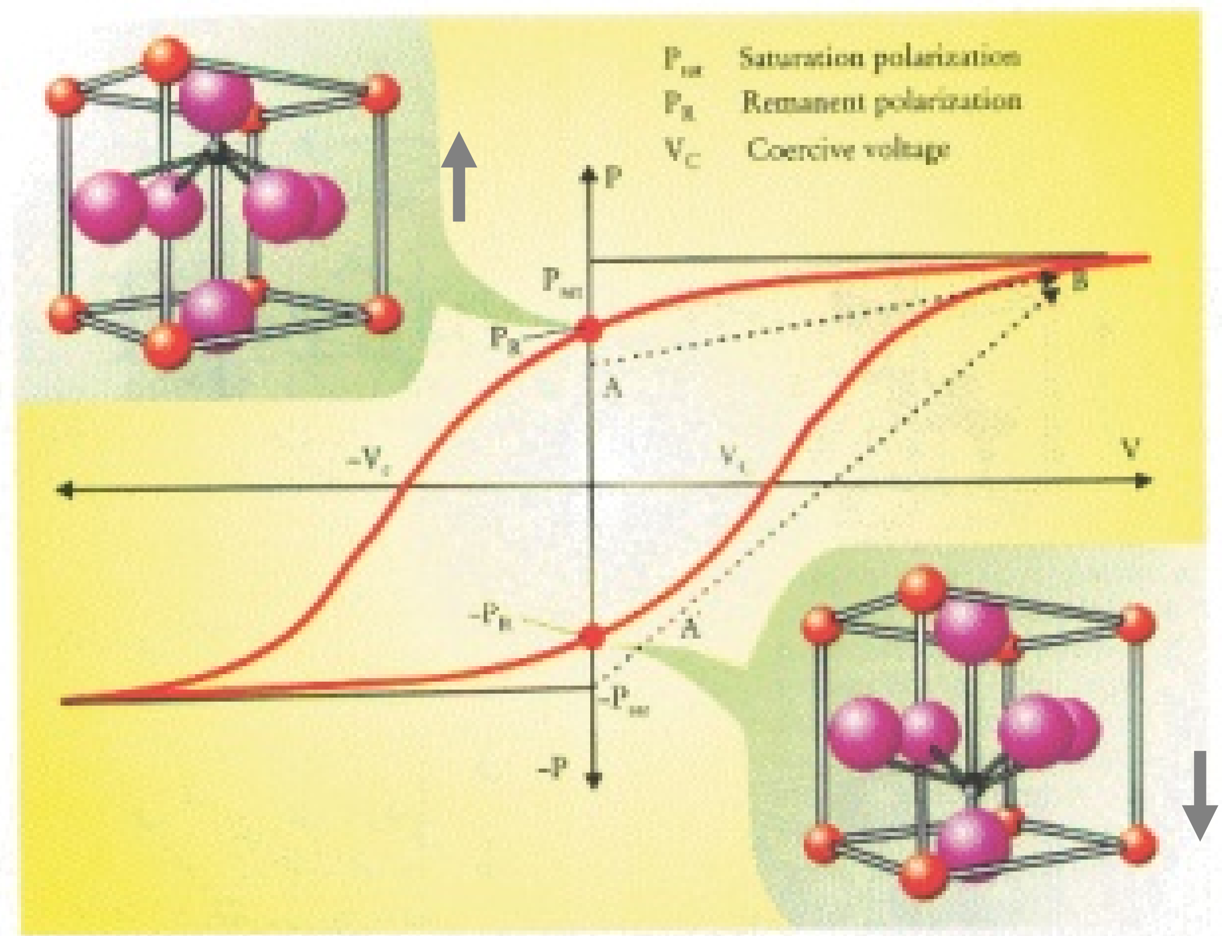

Superlattice Technology:
Laser ablation (1nm-1µm)

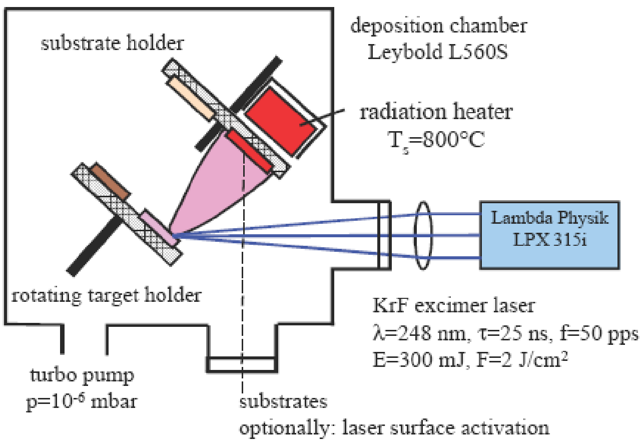

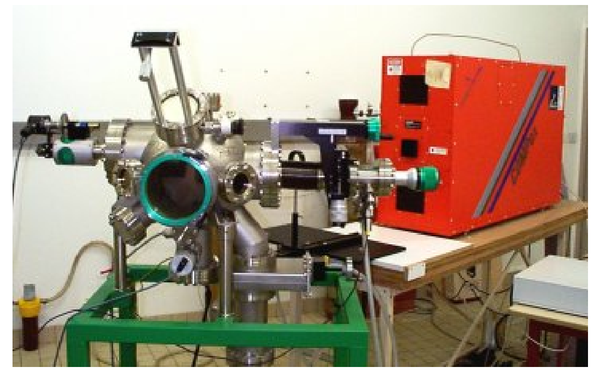

Result: Films ... and Multilayers

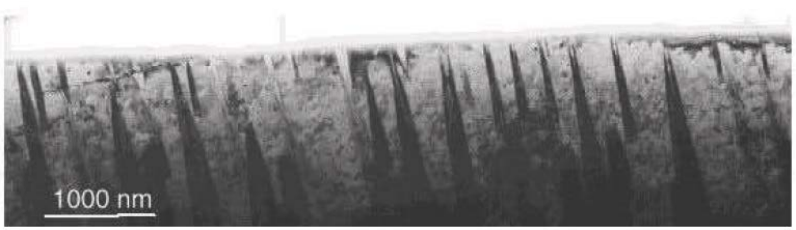

c/a/c/a 2-domain Structure (200 nm PZT 20/80 on $SrTiO_3$)

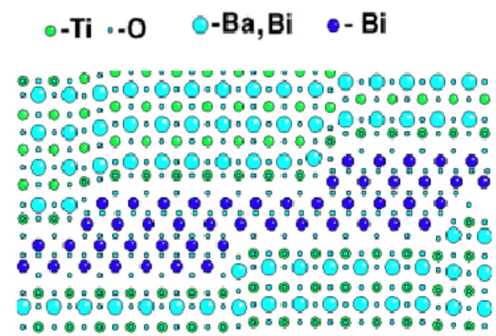

Nano-scale ?

Solid State Communications, Vol. 11, pp. 291–294, 1972. Pergamon Press.

THERMODYNAMIC STABILITY OF THIN FERROELECTRIC FILMS

I.P. Batra and B.D. Silverman

IBM Research Laboratory, San Jose, California

(*Received* 15 *March* 1972 *by H. Suhl*)

It is shown that the residual depolarization field in a ferroelectric thin film which arises from the incomplete cancellation of polarization and compensation charge in a semiconducting electrode, introduces modifications in the spontaneous polarization and transition temperature. It is also found that below a certain critical thickness the ferroelectric polar state is thermodynamically unstable. For triglycine sulphate the critical thickness is calculated to be 0.4 μm.

Periodic 180° Kittel domains

- were proposed by <u>Landau & Lifshitz</u> for ferromagnets in 1935

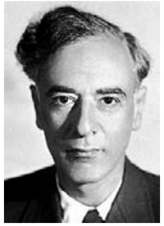

L. D. Landau and E. M. Lifshitz, Phys. Z. Sowjetunion 8, 153 (1935).

- were re-described by <u>Kittel</u> in 1946

C. Kittel, Phys. Rev. **70**, 965 (1946).

and …

… were forgotten for ferroelectrics till 2000's …

180° Ferroelectric domains

In theory…to minimize the energy of depolarization field E=-4πP

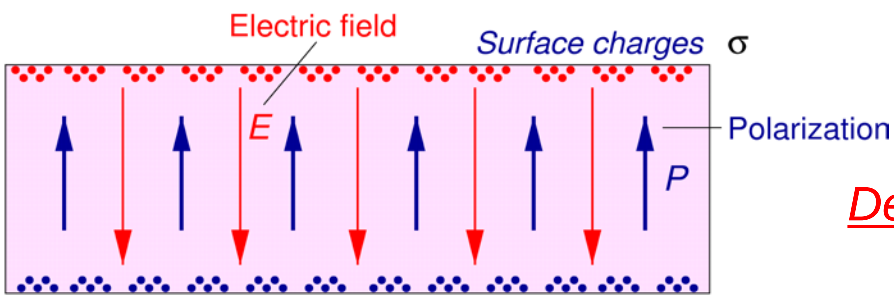

Mono-domain sample

<u>Depolarization energy</u> : $F_{dep} \sim \frac{E^2}{4\pi}$

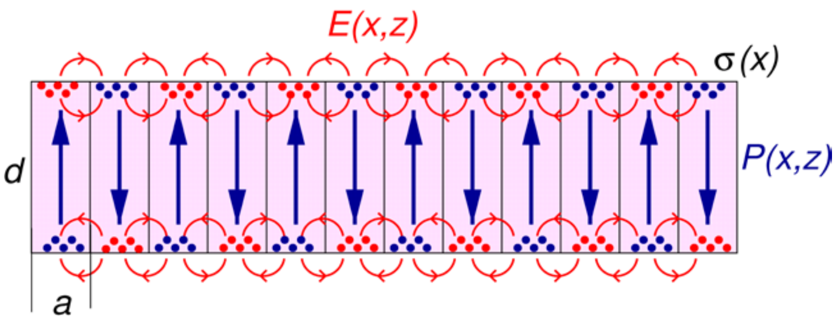

Multi-domain sample

Kittel *domains* are formed in c-oriented ferroelectric films and superlattices…

$PbTiO_3$

$SrTiO_3$

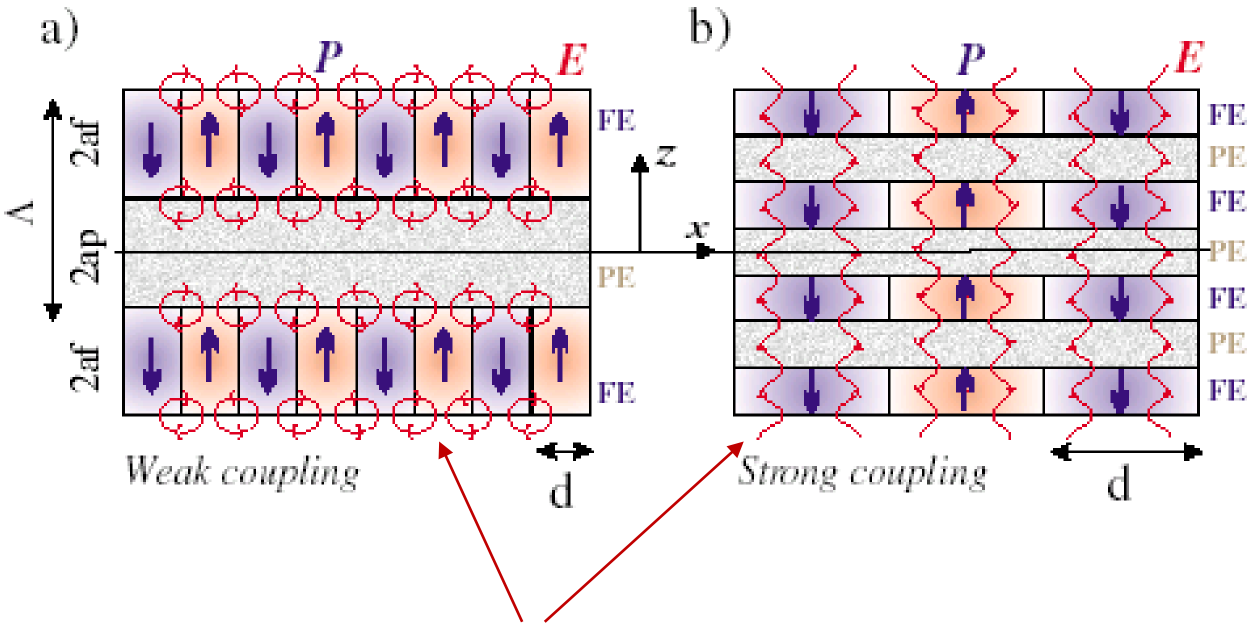

… to minimize the *depolarization field*

VA Stephanovich, IA Luk'yanchuk, MG Karkut, PRL 94 , 047601 (2005)
F De Guerville, I Luk'yanchuk, L Lahoche, M El Marssi Mat. Sci. & Eng. B 120, 16 (2005)
IA Luk'yanchuk, L Lahoche, A Sené, PRL 102, 147601 (2009)

X-Ray Diffraction Studies of 180° Ferroelectric Domains in $PbTiO_3/SrTiO_3$ Superlattices under an Applied Electric Field

P. Zubko,* N. Stucki, C. Lichtensteiger, and J.-M. Triscone

Experimental confirmation

Domain satellite !!!

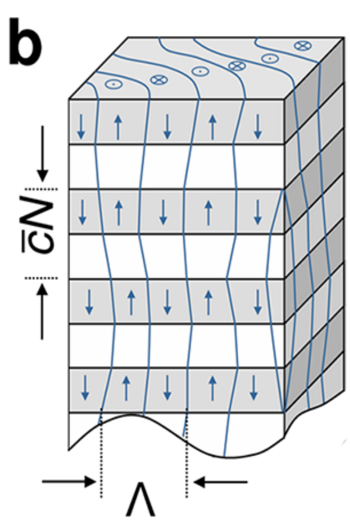

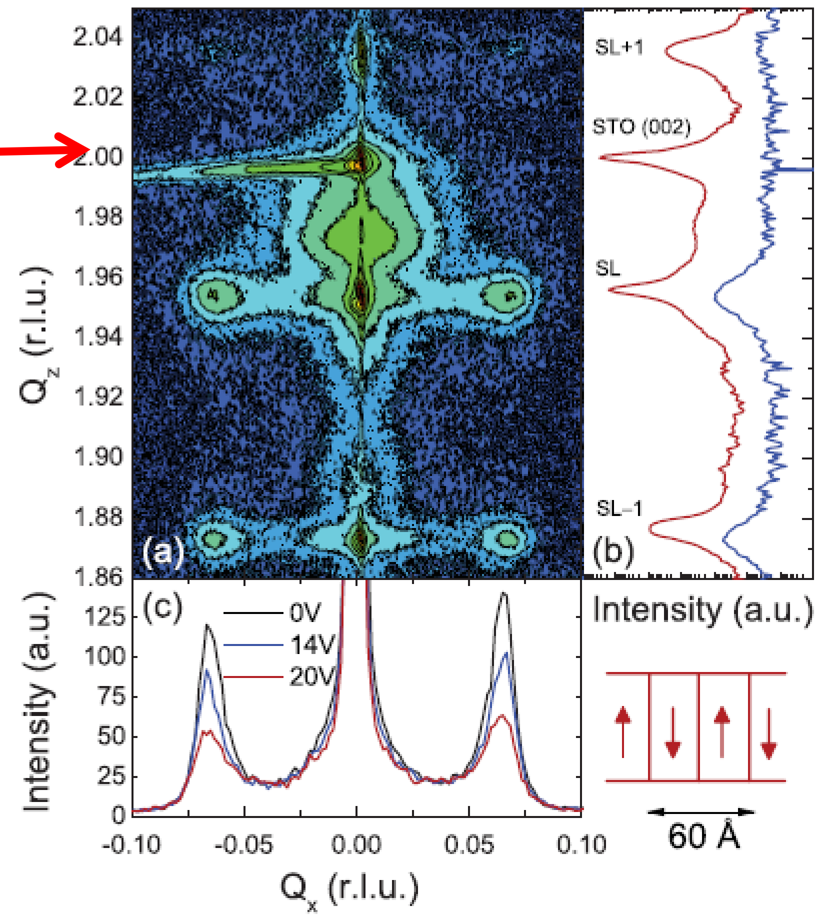

Advanced Photon Source
» an Office of Science User Facility

Imaging Ferroelectric Domains

JANUARY 29, 2014

SHARE

PbTiO3

When thin films of ferroelectric materials are grown on single-crystal substrates, they can develop regions of aligned polarization — called "domains" — that often adopt complex patterns. Manipulation of ferroelectric domains can lead to advances in a number of technologies. However, in order to manipulate the domains, it is important to study their natural development. Previous studies have shown that interfacial strain and electrical boundary conditions play a large role. Accurate measurements of the local polarization can help science learn more. By changing the properties of the substrate and the interfaces of the ferroelectric materials, one can control the size and shape of the domains and thus influence the behavior of the

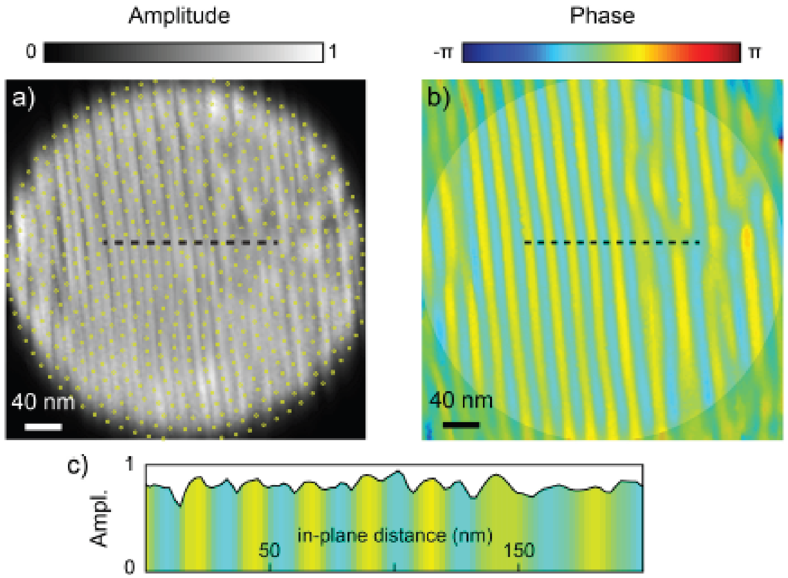

The striped domains of thin film lead titanate ($PbTiO_3$)

See: S.O. Hruszkewycz[1*], M.J. Highland[1], M.V. Holt[1], Dongjin Kim[1,2], C.M. Folkman[1], Carol Thompson[3], A. Tripathi[4], G.B. Stephenson[1], Seungbum Hong[1,2], and P.H. Fuoss[1], "Imaging Local Polarization in Ferroelectric Thin Films by Coherent X-Ray Bragg Projection Ptychography," Phys Rev.

Observation of polar vortices in oxide superlattices

A. K. Yadav[1,2]*, C. T. Nelson[1,3,4]*, S. L. Hsu[1,3,4], Z. Hong[5], J. D. Clarkson[1,3], C. M. Schlepütz[6], A. R. Damodaran[1], P. Shafer[7], E. Arenholz[7], L. R. Dedon[1], D. Chen[1,3], A. Vishwanath[2,3], A. M. Minor[1,2,4], L. Q. Chen[5], J. F. Scott[8], L. W. Martin[1,2] & R. Ramesh[1,2,3]

LETTER RESEARCH

198 | NATURE | VOL 530 | 11 FEBRUARY 2016

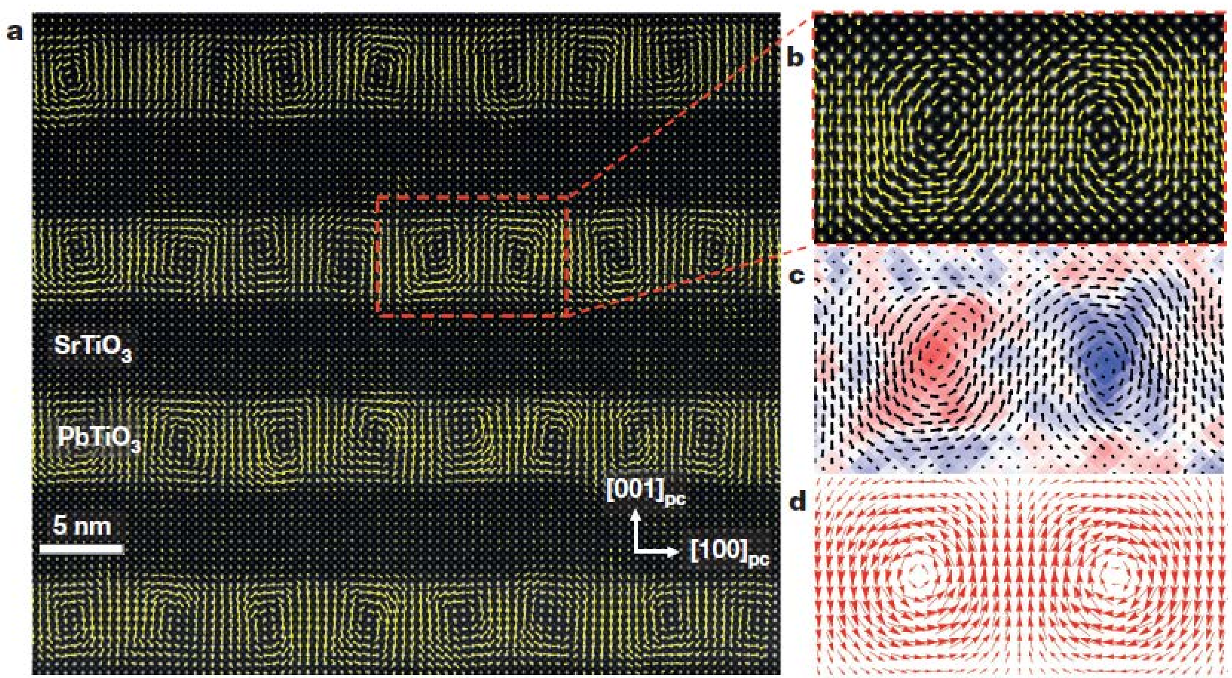

F De Guerville, I Luk'yanchuk, L Lahoche, M El Marssi Mat. Sci. & Eng. B 120, 16 (2005)
IA Luk'yanchuk, L Lahoche, A Sené, PRL 102, 147601 (2009)

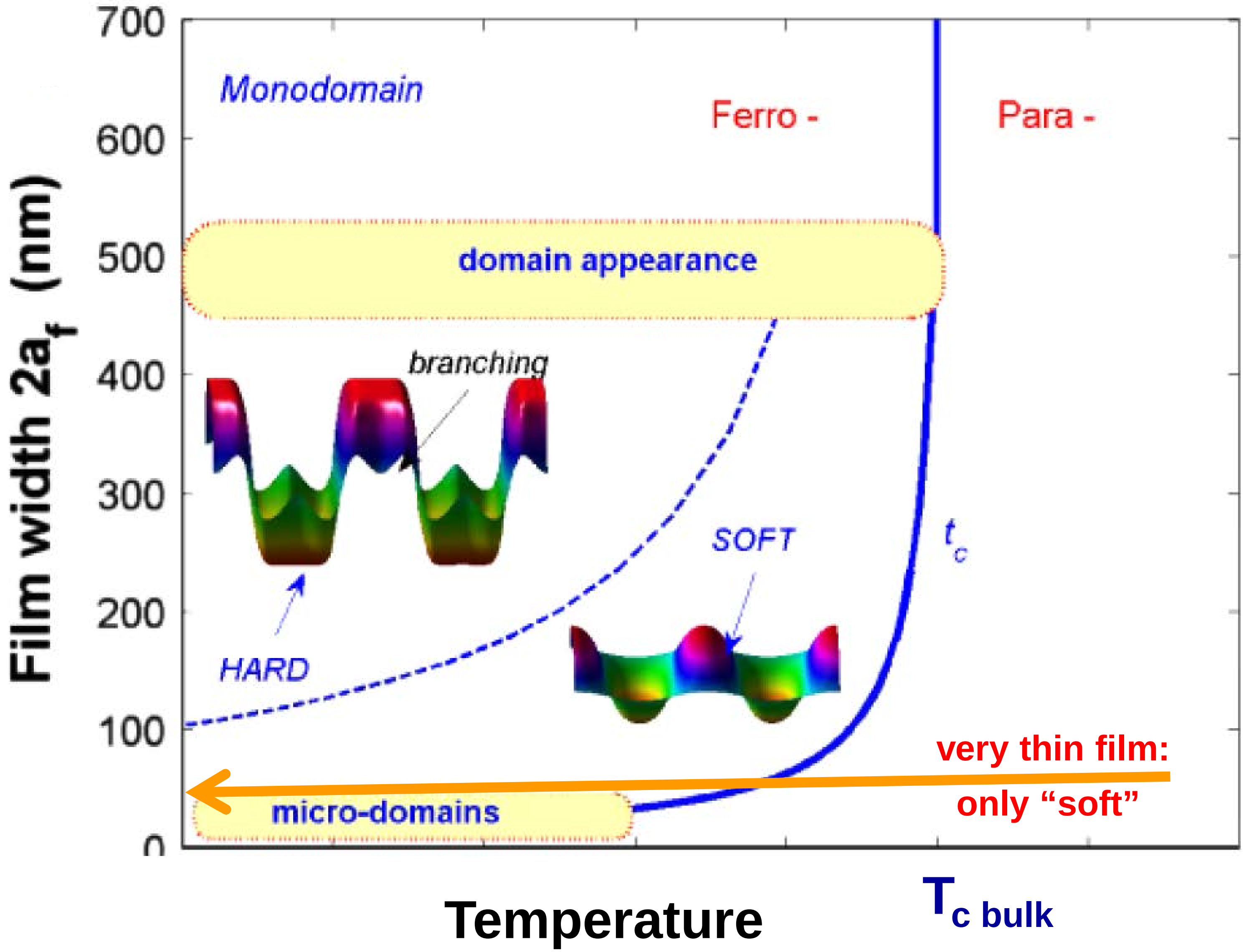

Soft domains

Gradual profile of spontaneous polarization
is described by …

$$\boldsymbol{P}(x,z) = A\, sn\, (k_1 x,\, m_1)\, sn\, (k_2 z, m_2)$$

(Lukyanchuk et al. 2009)

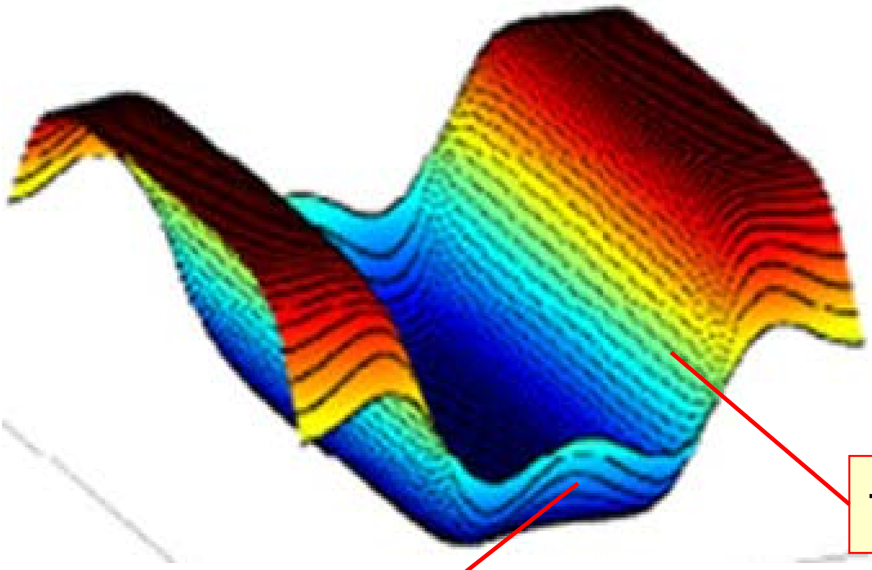

thick domain wall

Polarization vanishes
at the sample boundary

Hard (Kittel) domains, P=const

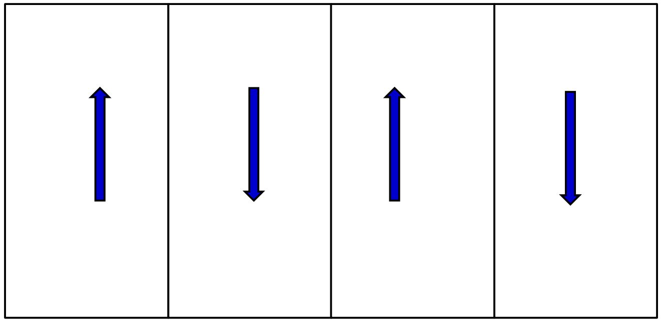

Soft domains, P=cos(kz)cos(qx)

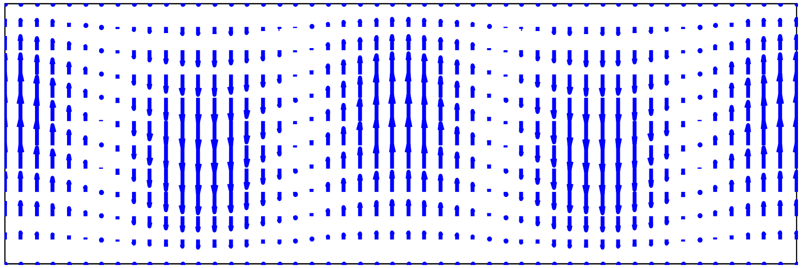

Landau Lifshitz paradox

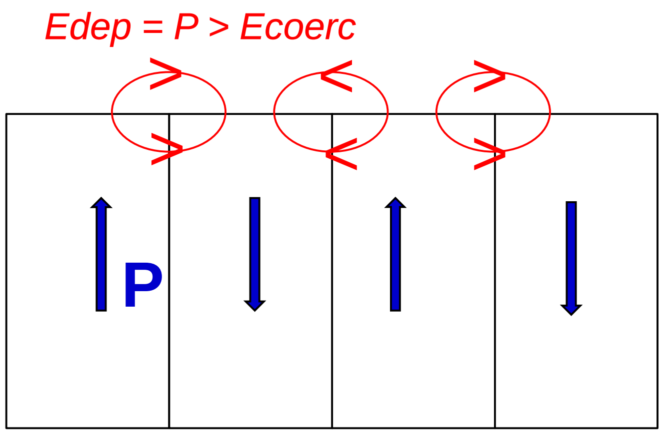

Fractal branching

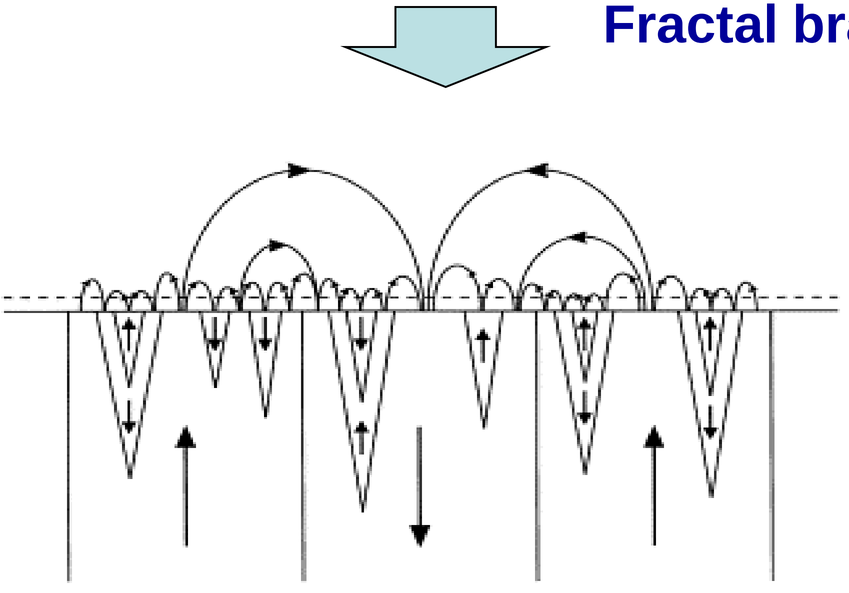

"soft" *spontaneous* polarization, $\mathbf{P}_0$ (z-component)

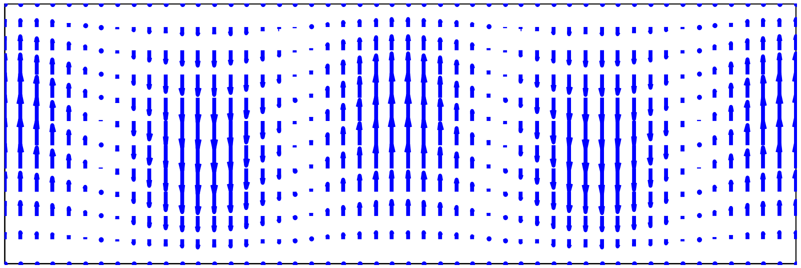

Very thin films
Soft domain

+ induced *depolarization* field, **E** (smaller)

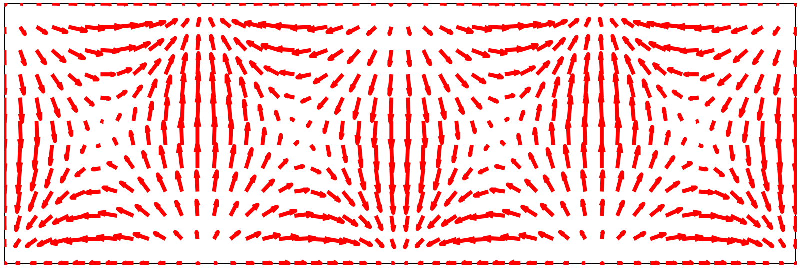

solution of…

$$(\partial_z^2 + \varepsilon_\perp \partial_x^2)\varphi^{(f)} = 4\pi \partial_z P.$$

“soft” *spontaneous* polarization, $\mathbf{P}_0$ (z-component)

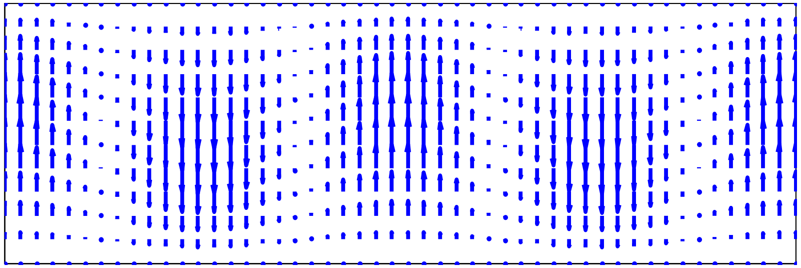

Very thin films
Soft domain
& vortex tubes

+ induced *depolarization* field, **E**

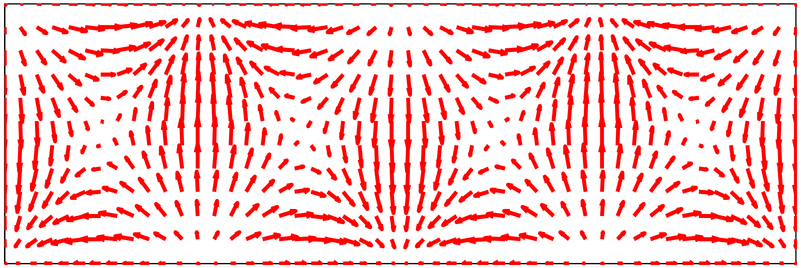

solution of…

$$(\partial_z^2 + \varepsilon_\perp \partial_x^2)\varphi^{(f)} = 4\pi\partial_z P.$$

= “vortices” of *total* polarization $\mathbf{P}=\mathbf{P}_0+\chi_\perp \mathbf{E}$

(*new state of matter*)

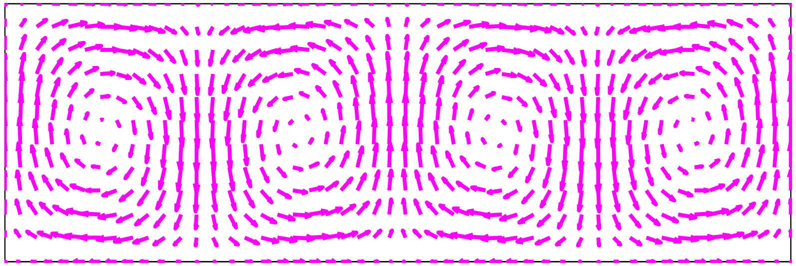

Negative capacitance

Can capacitance be negative ???

$$E = \frac{1}{2\,C} Q^2$$ ***impossible*?**

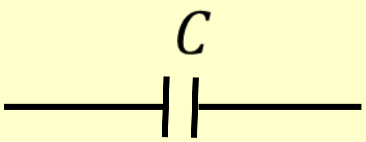

but…

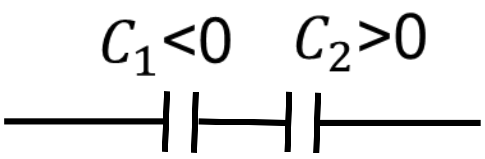

For two in-series capacitances

$$\frac{1}{C_{tot}} = \frac{1}{C_1} + \frac{1}{C_2}$$

$$C_{tot} = \frac{C_1 C_2}{C_1 + C_2}.$$

$$C_{tot} > 0$$

Useful application

for ultra-low-power nanoelectronics

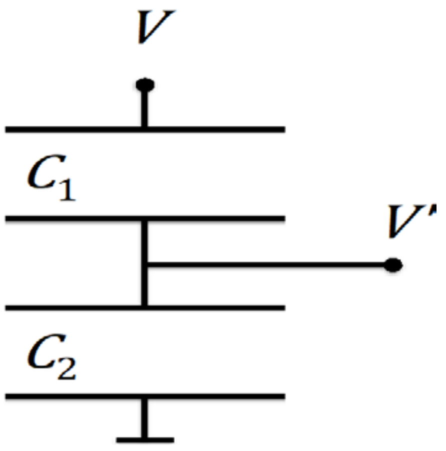

Voltage enhancement, if C_1<0

$$V' = \frac{1}{1 + C_2/C_1} V > V$$

Device implementation:

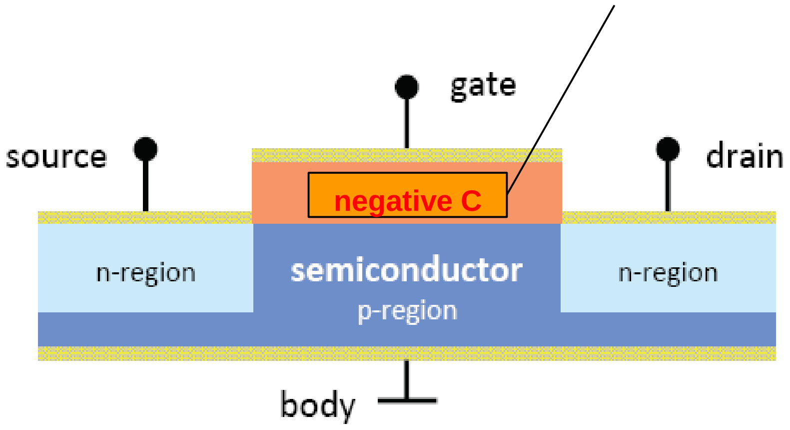

C: A. Cano and D. Jimenez, Appl. Phys. Lett. 97, 133509 (2010).

IN FERROELECTRICS:

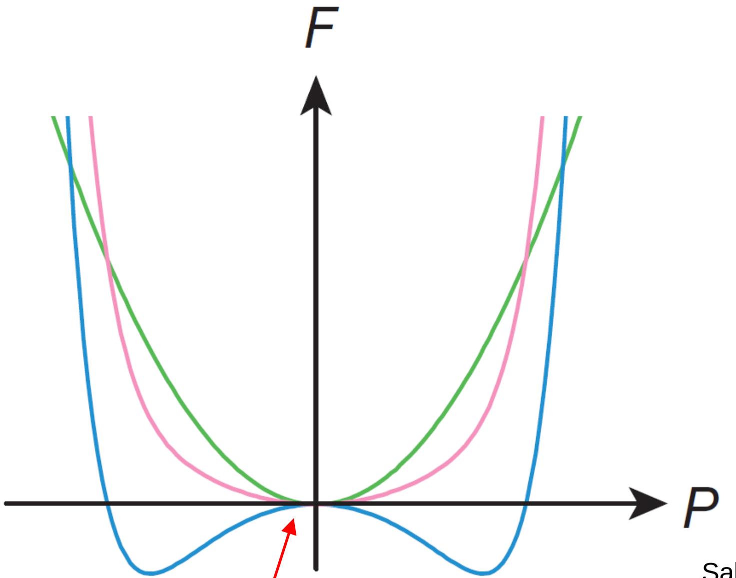

$$\varepsilon \propto \frac{\partial^2 F}{\partial P^2} < 0$$

monodomain

Salahuddin, S. & Datta, S. Use of Negative Capacitance to Provide Voltage Amplification for Low Power Nanoscale Devices. Nano Lett. 8, 405-410 (2008).

Zhirnov, V. V. & Cavin, R. K. Negative capacitance to the rescue? Nature Nanotechnology 3, 77-78 (2008).

A. Cano and D. Jimenez, Multidomain ferroelectricity as a limiting factor for voltage amplification in ferroelectric field-effect transistors, Appl. Phys. Lett. 97, 133509 (2010).

Krowne, C. M., Kirchoefer, S. W., Chang, W., Pond, J. M., & Alldredge, L. M. B. Examination of the possibility of negative capacitance using ferroelectric materials in solid state electronic devices. Nano letters, 11(3), 988-992. (2011).

Appleby, D. J. R., Ponon, N. K., Kwa, K. S. K., et al. Experimental Observation of Negative Capacitance in Ferroelectrics at Room Temperature. Nano Lett. 14, 3864-3868 (2014).

Gao, W., Khan, A., Marti, X., Nelson, C., Serrao, C., Ravichandran, J., ... & Salahuddin, S. (Room-temperature negative capacitance in a ferroelectric–dielectric superlattice heterostructure. Nano letters, 14(10), 5814-5819. 2014).

Khan AI, Chatterjee K, Wang B, Drapcho S, You L, Serrao, C, Bakaul SR, Ramesh R, and Salahuddin S. Negative capacitance in a ferroelectric capacitor. Nature Materials 14, 182–186 (2015).

Catalan, G., Jim´enez, D. & Gruverman, A. Negative capacitance detected. Nature Materials. 14, 137-139 (2015)

Temperature dependence $\varepsilon(T) < 0$ *

P. Zubko, J.C. Wojdeł, M. Hadjimichael, S. Fernandez-Pena, A. Sené, I. Luk'yanchuk, J.-M. Triscone, J. Íñiguez, Nature, 534, 524 (2016)

A. Sené, MSc Thesis (2007), PhD Thesis (2010)

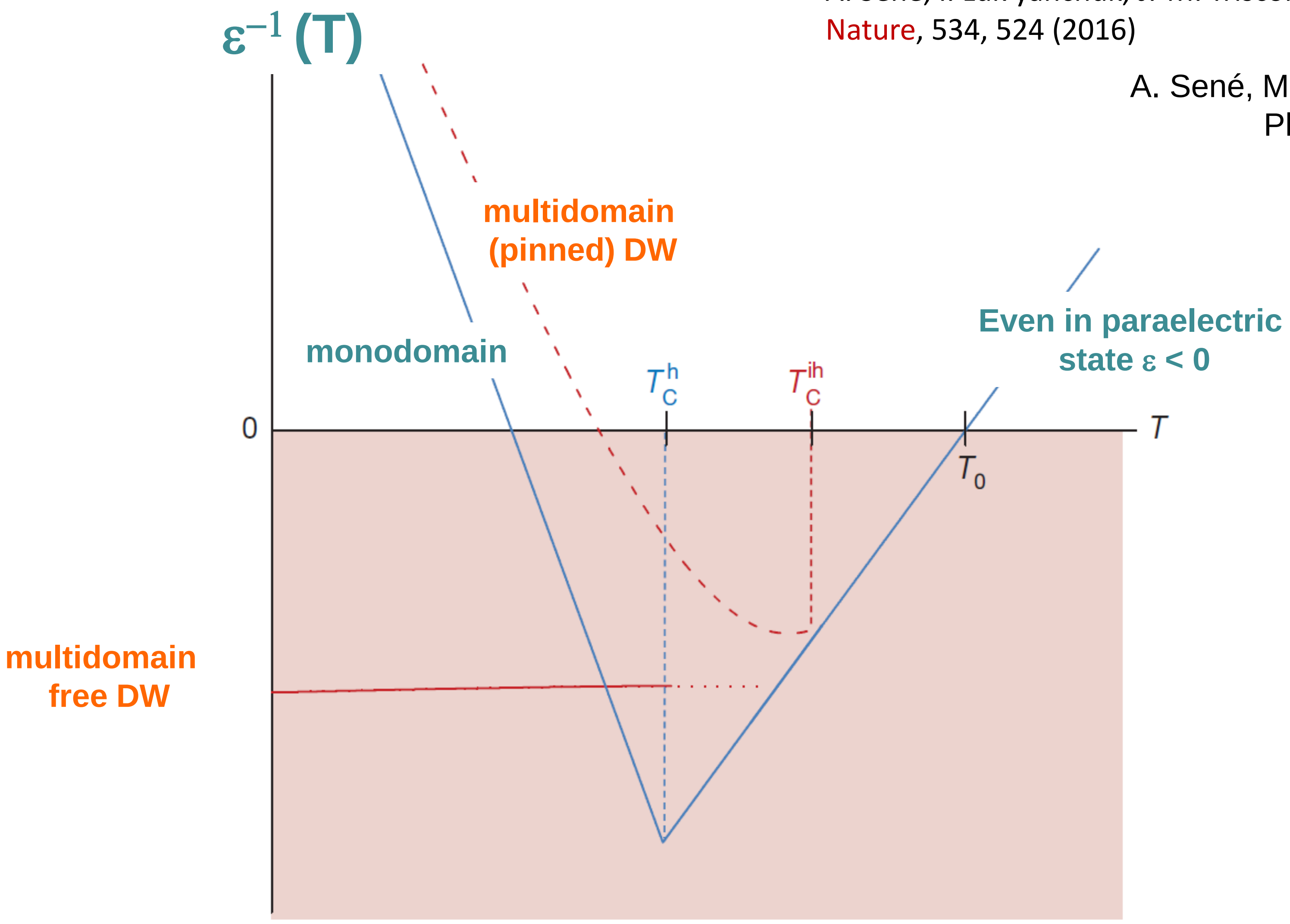

ε(T)<0 , direct experimental observation, 2016

Negative Capacitance in Multidomain Ferroelectric Superlattices,
P. Zubko, J.C. Wojdeł, M. Hadjimichael, S. Fernandez-Pena, A. Sené, **I. Luk'yanchuk**, J.-M. Triscone, J. Íñiguez,
Nature, 534, 524 (2016)

X-ray

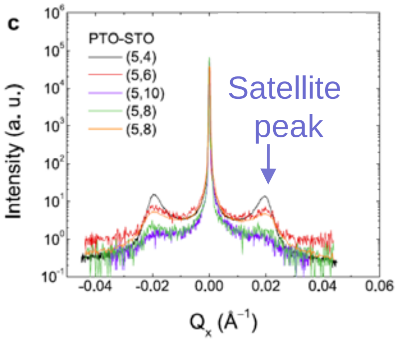

Domains are here !

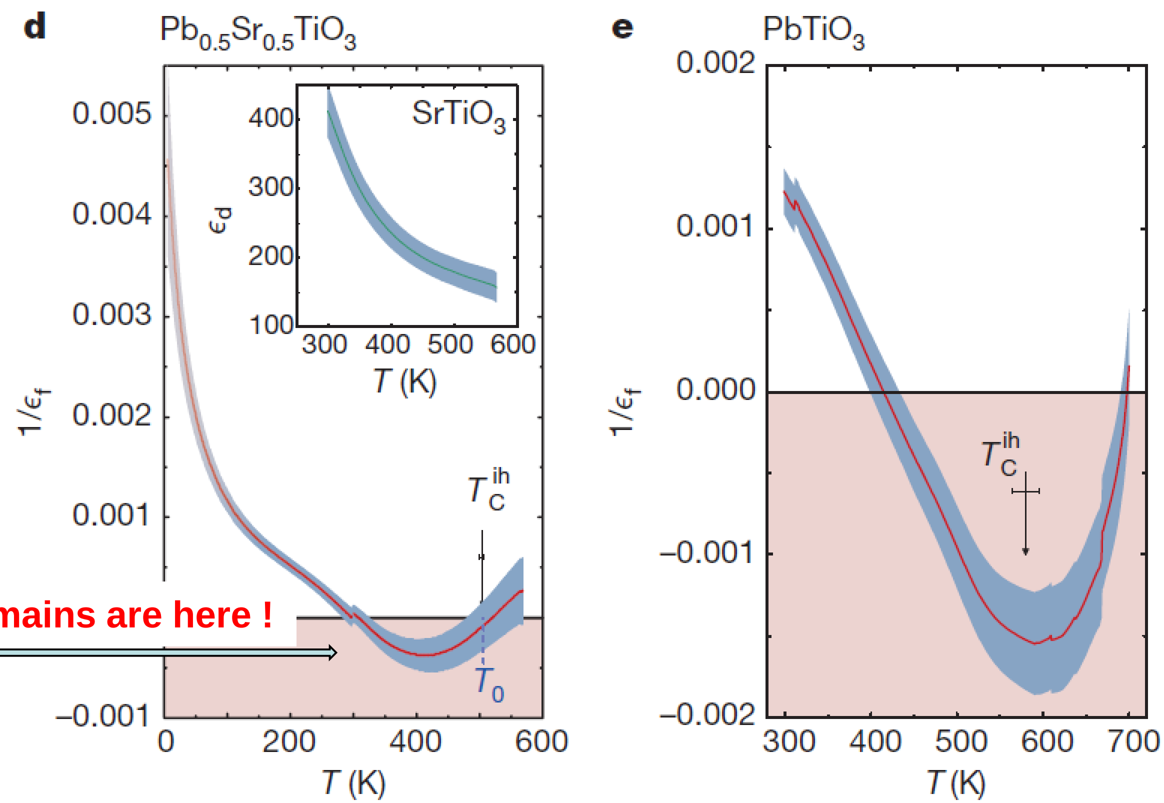

Figure 2 | Temperature dependence of the dielectric permittivities of $Pb_{0.5}Sr_{0.5}TiO_3$–$SrTiO_3$ and $PbTiO_3$–$SrTiO_3$ superlattices.

ε(T)<0 , ab-initio monte-carlo simulations, 2016

(ibid.)

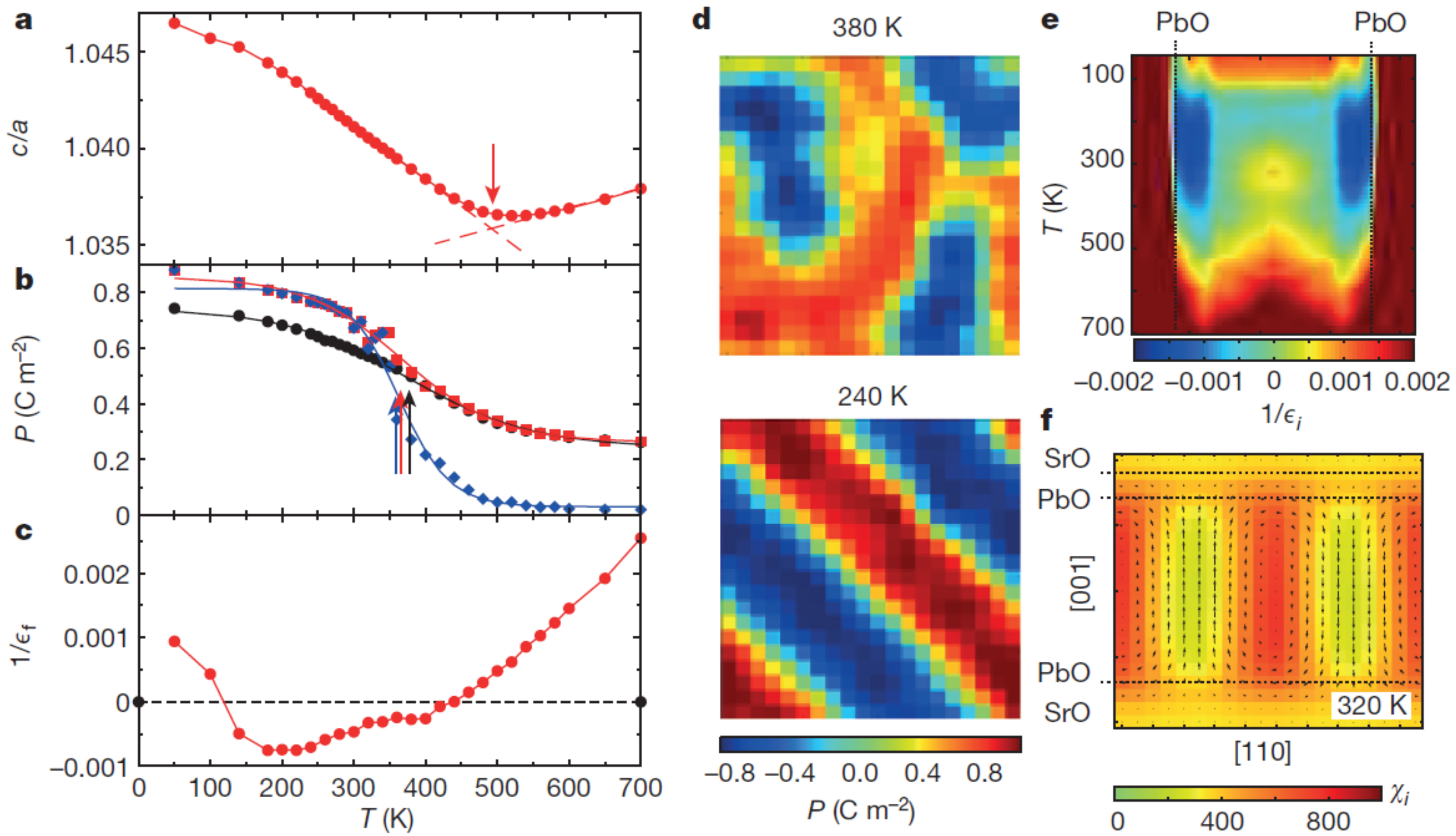

PbTiO3

Why ε is negative?

In external field, *D = ε E*

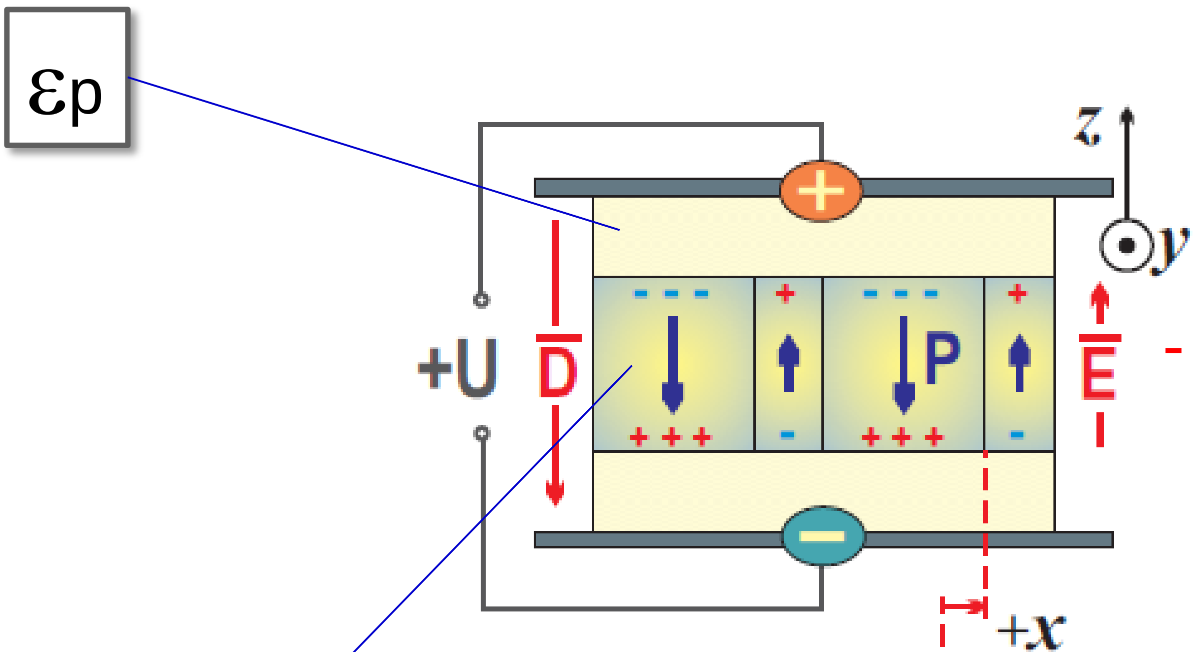

- **opposite to P and D !!!**

$$\varepsilon_f = \varepsilon_{\|} - \frac{\pi}{2\ln 2}\left(\frac{\varepsilon_{\perp}}{\varepsilon_{\|}}\right)^{1/2}\frac{2a_f}{d}\varepsilon_{\|} < 0$$

Intrinsic

DW motion, Negative !!

A.M. Bratkovsky and A.P. Levanyuk, 2001

A. Kopal, P. Mokry, J. Fousek T. Bahnık 1999

THz dynamics of domain walls

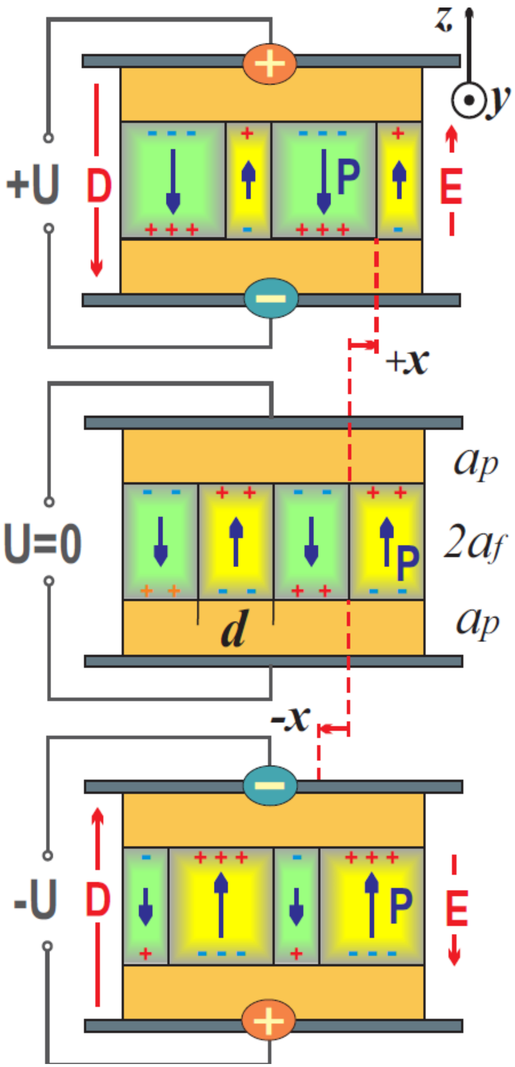

Domain dynamics
in applied
$E(t) = E_0 \cos(\omega t)$

What is the dynamical dielectric response

$\varepsilon(\omega)$???

Principal result

Dispersion ε(ω) for PTO layer

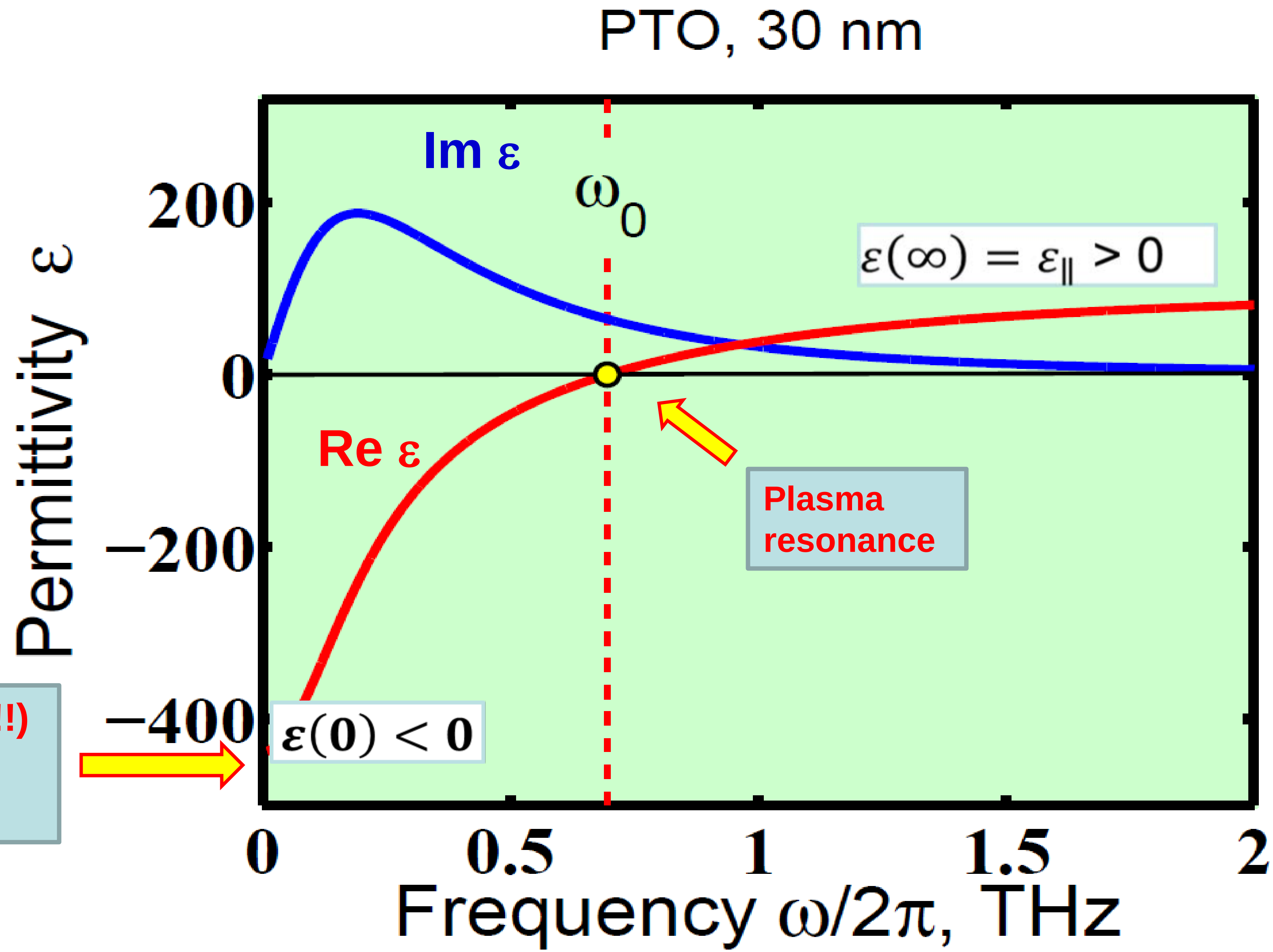

Negative (!!) due to DW motion

Different from ε(ω) in FIR
of polar molecules, soft mode …

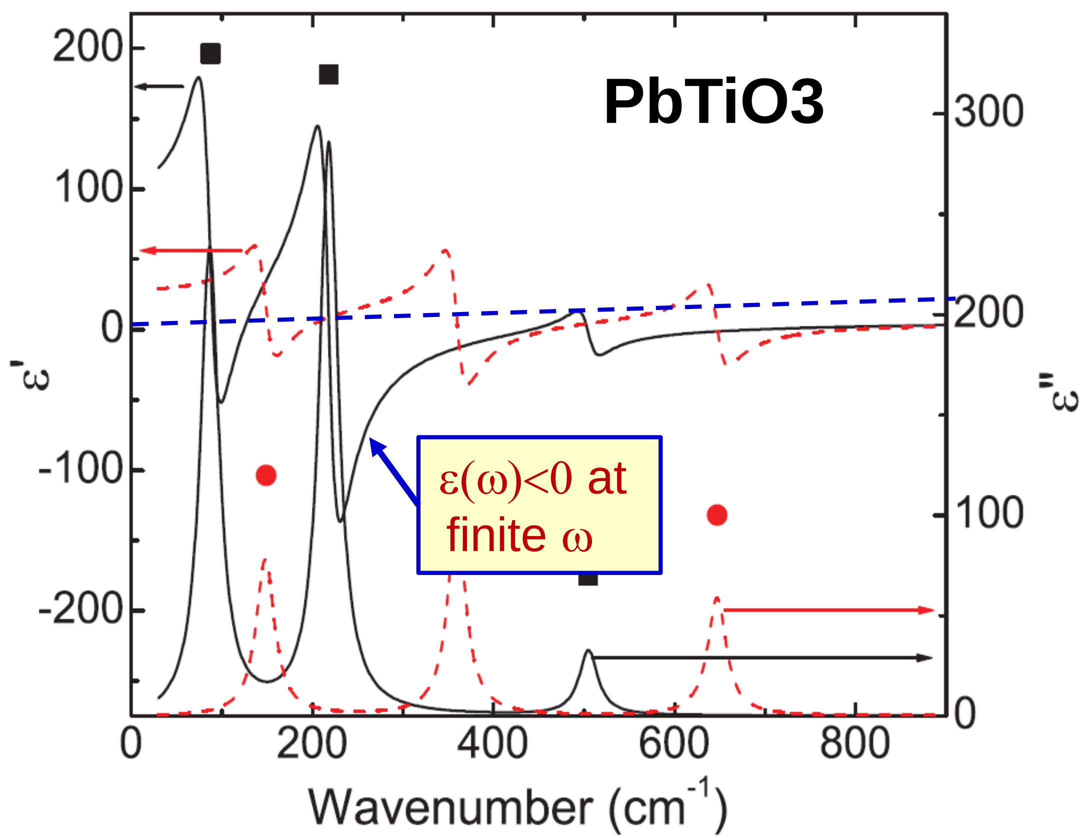

Hlinka, J., Simon, E., Bogicevic, C., Karolak, F. & Janolin, P. E. Phys. Rev. B 84, 092104 (2011)

… *Déjà vu*

plasma oscillations in metal

Introduction to
Solid State Physics

CHARLES KITTEL

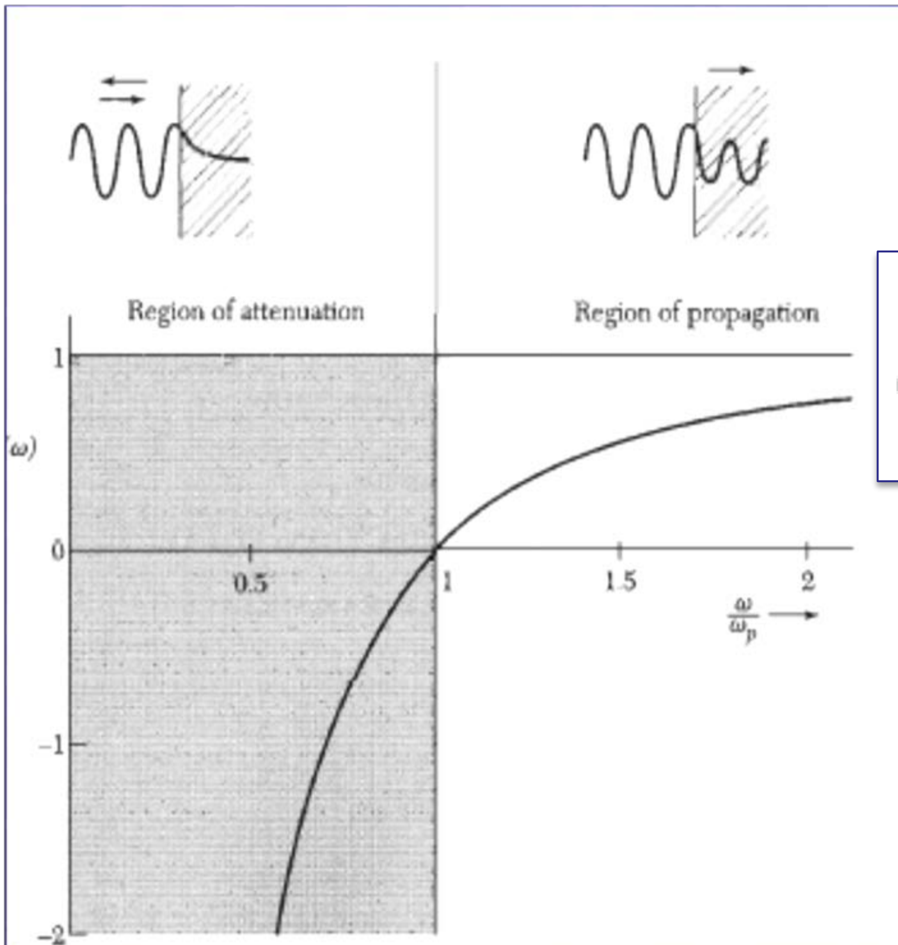

$$\epsilon(\omega) = 1 - \frac{\omega_p^2}{\omega^2}$$

Plasma resonance

In metal

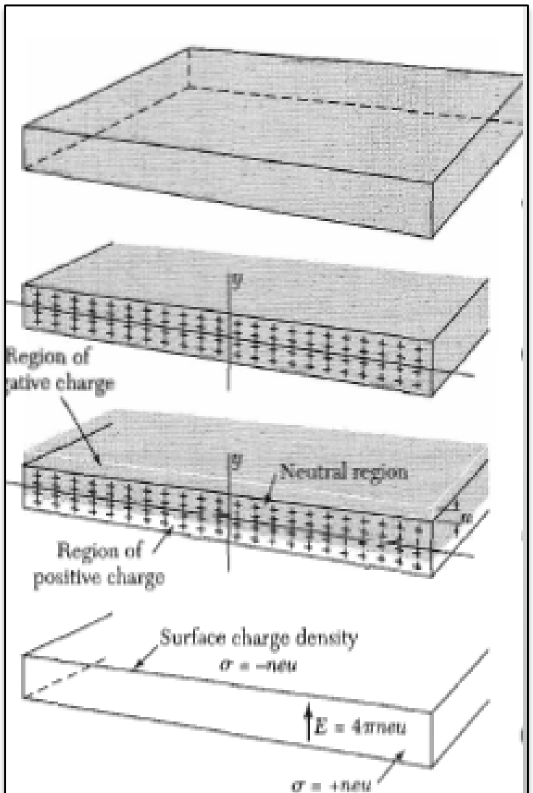

At UV frequency

In ferroelectric with DW

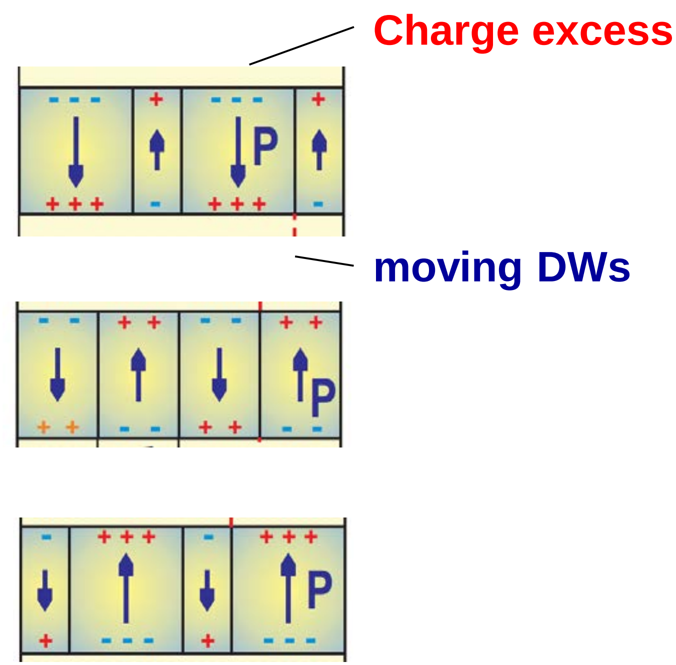

At sub-THz frequency

Electrodynamics

(plasmonics)

DW plasma resonance

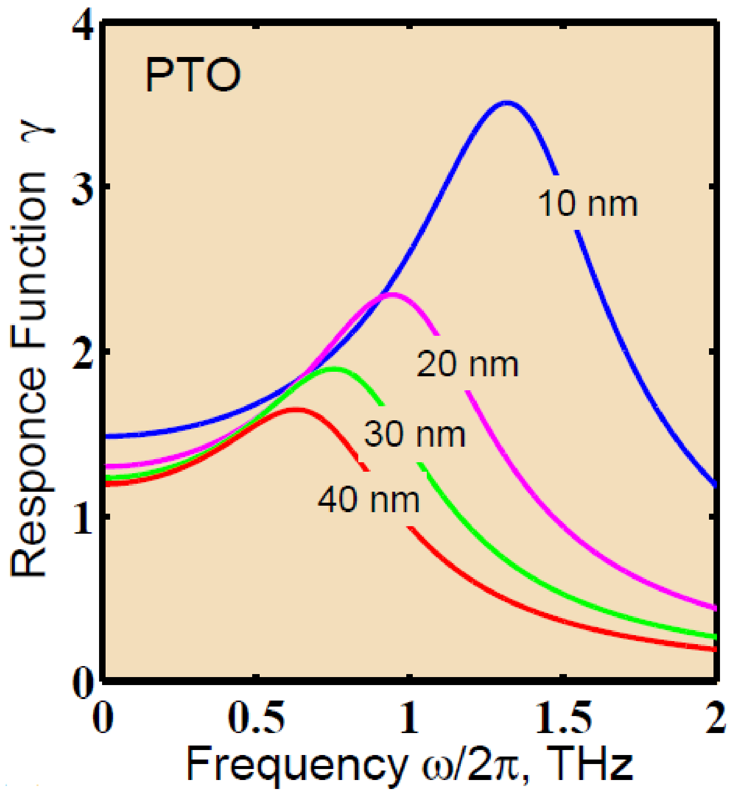

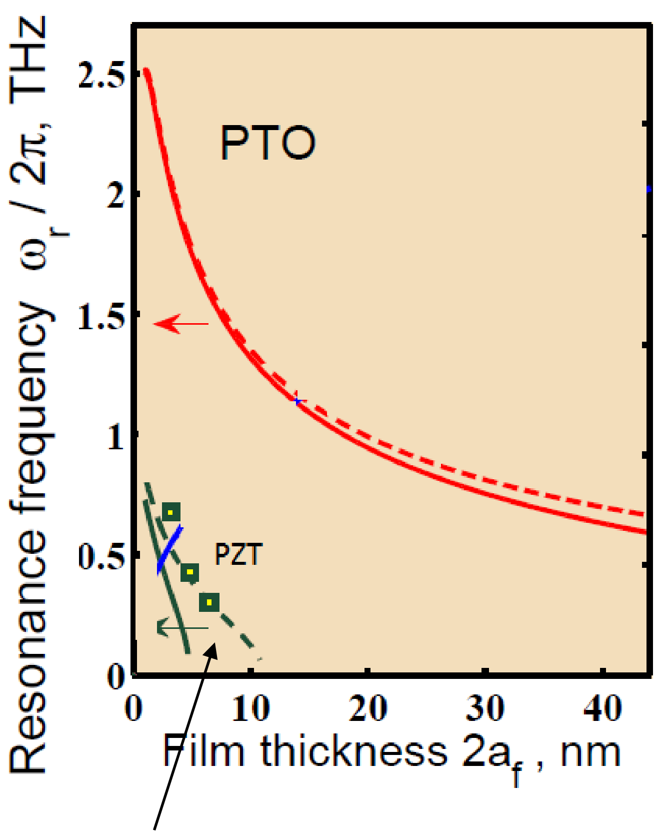

PZT, ab-initio:
Q. Zhang, R. Herchig,
I. Ponomareva 2011

Model: harmonic oscillator

$$\mu\ddot{x}(t) + \eta\dot{x}(t) + kx(t) = 2P_s E(t)$$

$$\mu \simeq 2.9 \cdot 10^{-9}\ \mathrm{kg/m^2}$$

Kittel model + ab-initio

Soft Mode damping

$$\tau \simeq 0.27\,\mathrm{ps}$$

$$k = \frac{4P_s^2}{d\varepsilon_0\varepsilon_{||}} g(z)$$

Deploarization restoring force

Dynamic response

$$\overline{\mathbf{P}}_{dw\,\omega} = \gamma(\omega)\,\overline{\mathbf{D}}_{\omega}$$

$$\gamma(\omega) = \frac{\gamma_0\,\omega_0^2}{\omega_0^2 - \omega^2 - i\Gamma\omega}; \quad \gamma_0 = \frac{4P_s^2}{\varepsilon_0\varepsilon_{||}kd} = \frac{1}{g(z)}$$

Size dependent !!!

With

$$\omega_0 = \sqrt{\frac{k}{\mu}} = \sqrt{\frac{4P_s^2}{\mu d\varepsilon_0\varepsilon_{||}}g(z)} \simeq \Omega_0\left(\frac{2\xi_0}{2a_f}\right)^{1/4}\left[1 - \frac{\ln 2}{2z}\right]$$

Material dependent !!!

and

$$z = \frac{\pi}{2}\sqrt{\frac{\varepsilon_{\perp}}{\varepsilon_{||}}}\frac{2a_f}{d}$$

$$\Omega_0 = \frac{2\varsigma^{-1/4}}{\varepsilon_{||}^{3/8}\varepsilon_{\perp}^{1/8}}\sqrt{\frac{P_s^2}{\mu\varepsilon_0\,2\xi_0}}.$$

Dispersion ε(ω) for PTO monolayer

$$\varepsilon_f = D/\varepsilon_0 E = \frac{\varepsilon_{\|}}{1-\gamma(\omega)}$$

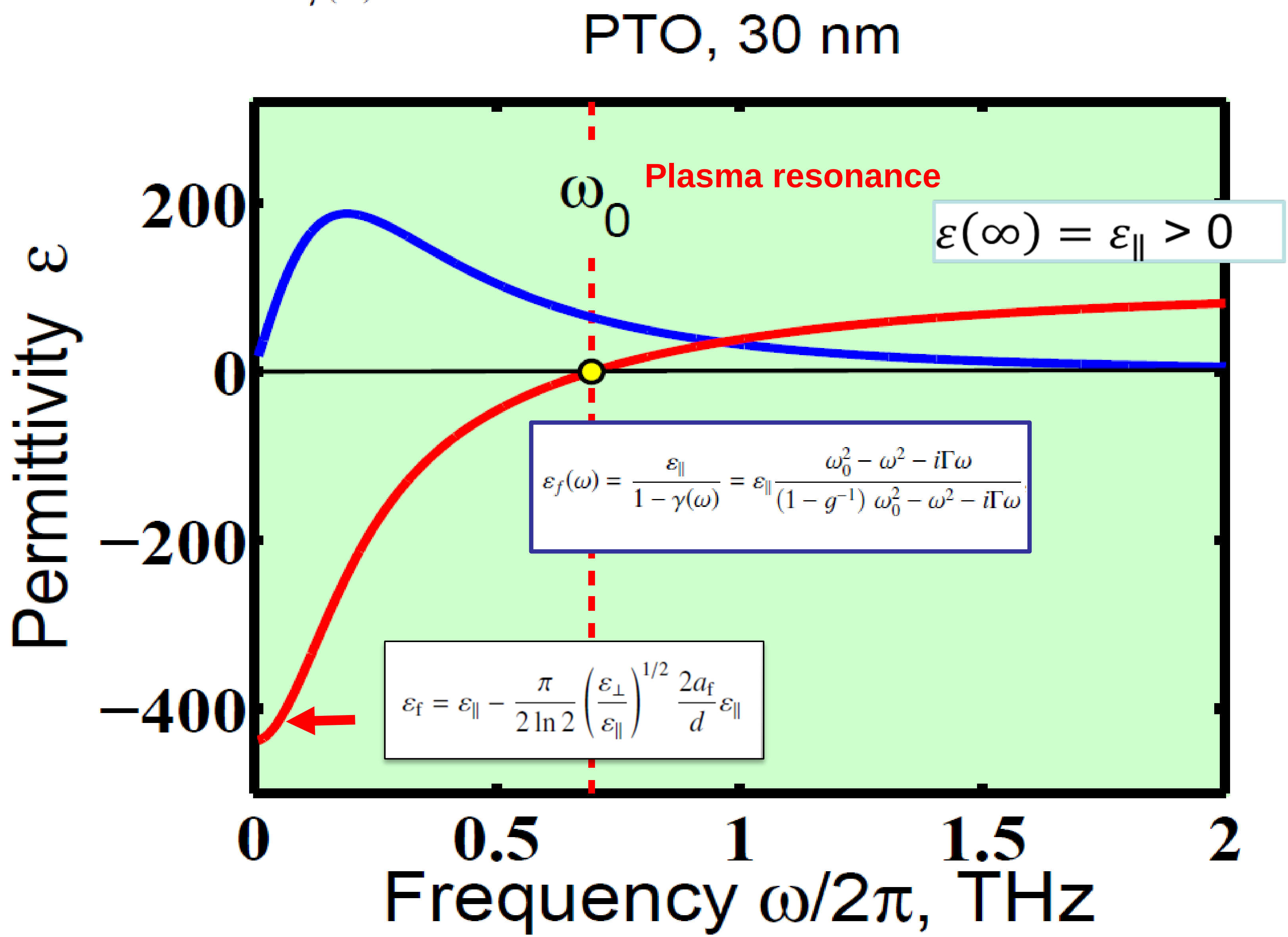

“By design”

Dynamic permittivity of para / ferro superlattice:

$$\varepsilon_{\text{tot}}^{-1}(\omega) = \alpha_{\text{p}}\varepsilon_{\text{p}}^{-1} + \alpha_{\text{f}}\varepsilon_{\text{f}}^{-1}(\omega)$$

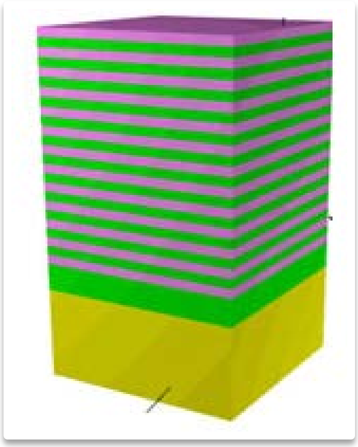

$$\varepsilon_{\text{tot}}(\omega) = \frac{\omega_{LO}^2 - \omega^2 - i\Gamma\omega}{\omega_{TO}^2 - \omega^2 - i\Gamma\omega}\varepsilon_{\text{tot}}(\infty)$$

with

$$\omega_{TO}^2/\omega_{LO}^2 = \varepsilon_{\text{tot}}(\infty)/\varepsilon_{\text{tot}}(0)$$

$$\varepsilon_{\text{tot}}^{-1}(0) = \alpha_{\text{p}}\varepsilon_{\text{p}}^{-1} + \alpha_{\text{f}}\varepsilon_{\text{f}}^{-1}$$

$$\varepsilon_{\text{tot}}^{-1}(\infty) = \alpha_{\text{p}}\varepsilon_{\text{p}}^{-1} + \alpha_{\text{f}}\varepsilon_{||}^{-1}$$

PTO-STO superlattice: *THz (NEZ) Metamaterial*

$$\frac{1}{\overline{\varepsilon}(\omega)} = \frac{\alpha_p}{\varepsilon_p} + \frac{\alpha_f}{\varepsilon_f(\omega)}$$

Tuning of ε(ω) !!!

positive

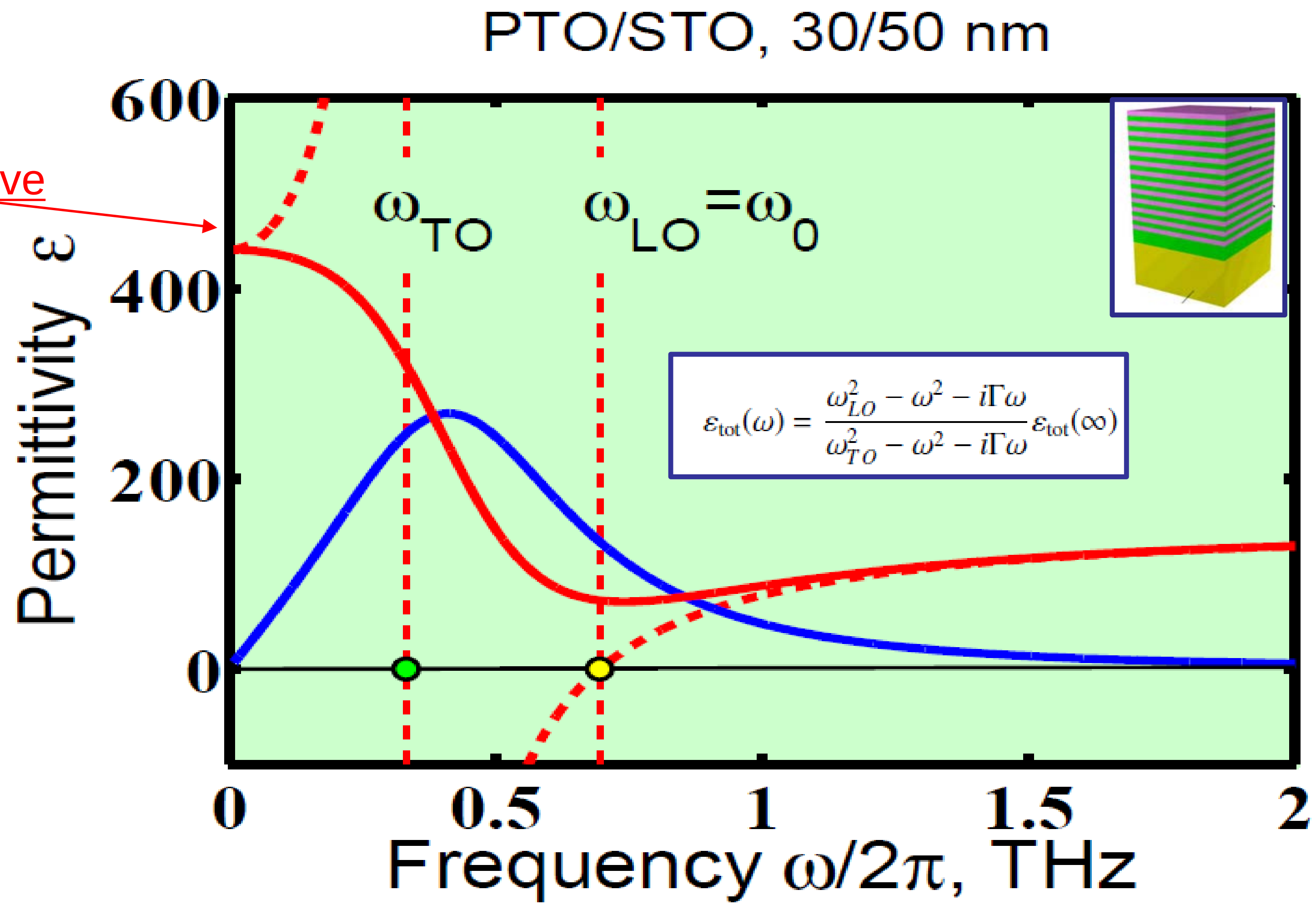

THz Optics, How to detect ???

with

$$\varepsilon_f(\omega) = \frac{\varepsilon_{\parallel}}{1-\gamma(\omega)} = \varepsilon_{\parallel}\frac{\omega_0^2 - \omega^2 - i\Gamma\omega}{(1-g^{-1})\,\omega_0^2 - \omega^2 - i\Gamma\omega}$$

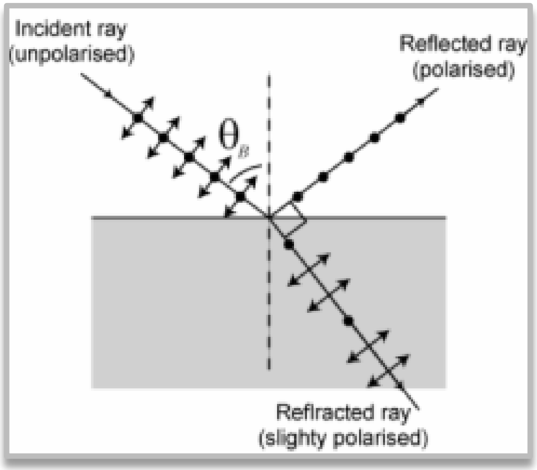

Refractive index:

$$n(\omega) = \sqrt{\varepsilon(\omega)}$$

p-Reflectivity:

$$R^{(p)}(\omega) = \left|\frac{\varepsilon(\omega)\cos\theta - \sqrt{\varepsilon(\omega) - \sin^2\theta}}{\varepsilon(\omega)\cos\theta + \sqrt{\varepsilon(\omega) - \sin^2\theta}}\right|$$

Sub- and low THz Reflection-Absorbtion Spectroscopy (RAS)

Reflectance, p-polarization:

$$R^{(p)} \approx R_0^{(p)} \left| 1 - \frac{2a_f}{\lambda} \frac{8\pi \cos\theta \sin^2\theta}{\left(\cos\theta - \varepsilon_p^{-1/2} \sin\theta\right)^2} \mathrm{Im} \frac{1}{\varepsilon_f(\omega)} \right|$$

$$R_0^{(p)} = \left| \frac{\varepsilon_p \cos\theta - \sqrt{\varepsilon_p - \sin^2\theta}}{\varepsilon_p \cos\theta + \sqrt{\varepsilon_p - \sin^2\theta}} \right|^2$$

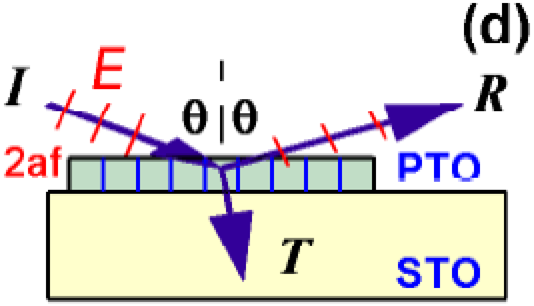

Observation of Giant Sub THz rezonance at Brewster angle

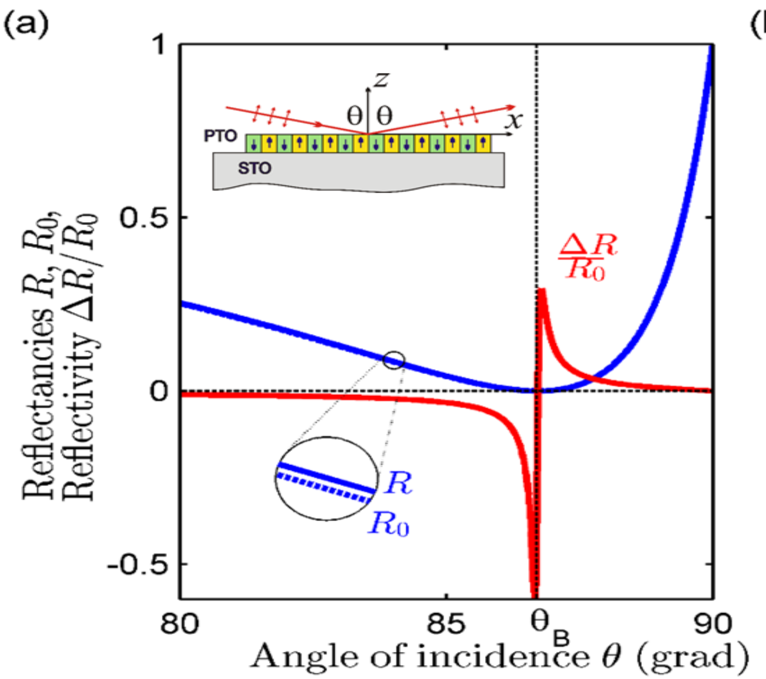

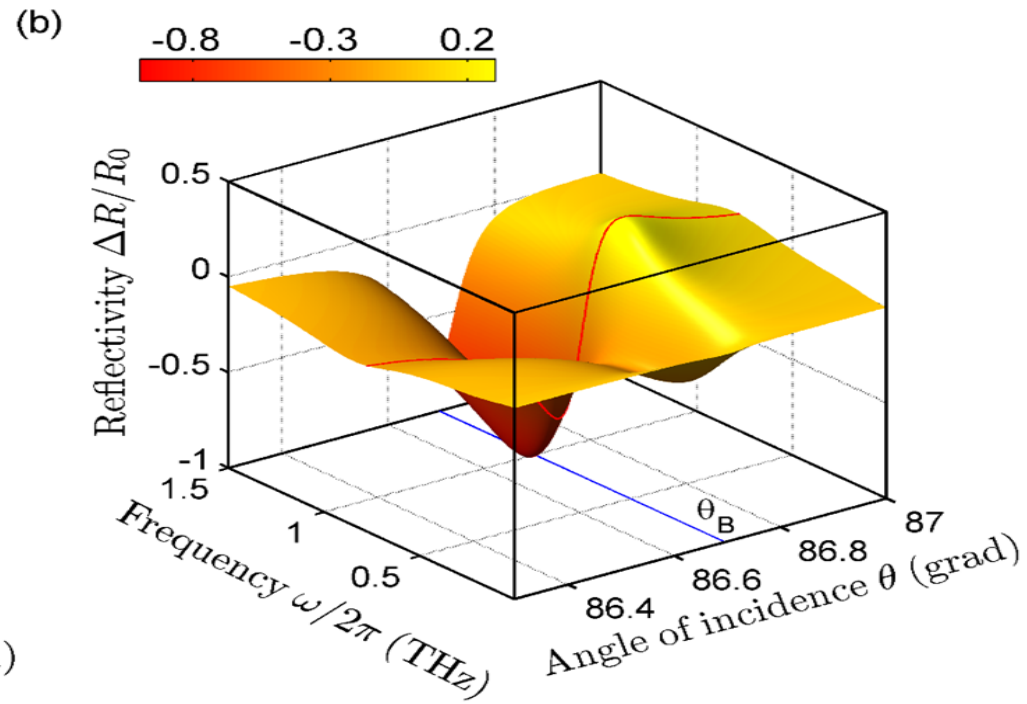

Giant effect for superlattices x10 !!!

Switching of Topological Structures in Ferroelectric nano-dots:

Domains, Vortices and Skyrmions

Electrostatics is important …

Multibit Logic

Ferroelectric symmetry-protected multibit memory cell

Laurent Baudry[1], Igor Lukyanchuk[2] & Valerii M. Vinokur[3]

SCIENTIFIC REPORTS

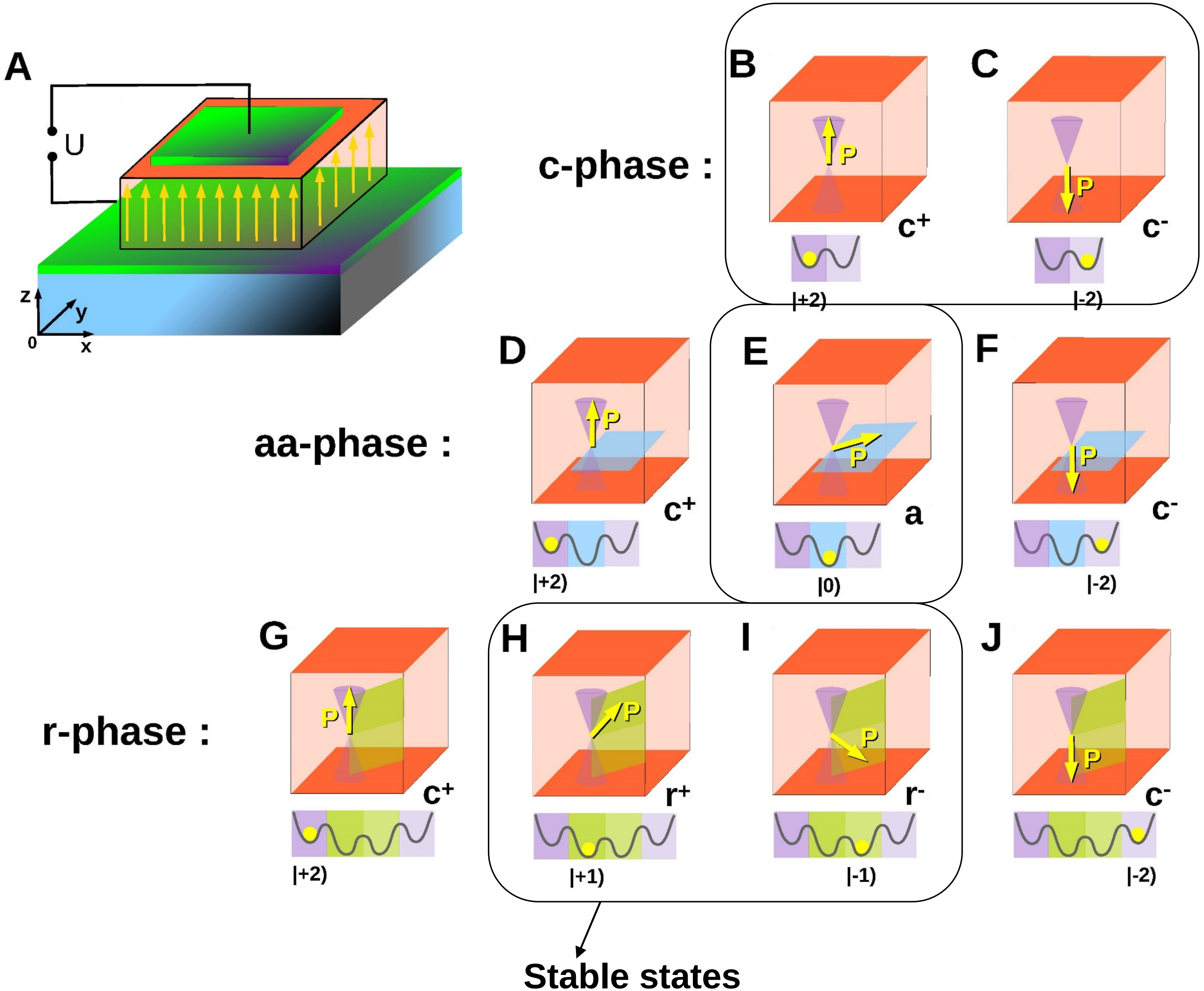

A
U
z
y
0
x
c-phase :
B
P
c+
|+2)
C
P
c-
|-2)
aa-phase :
D
P
c+
|+2)
E
P
a
|0)
F
P
c-
|-2)
r-phase :
G
P
c+
|+2)
H
P
r+
|+1)
I
P
r-
|-1)
J
P
c-
|-2)
Stable states

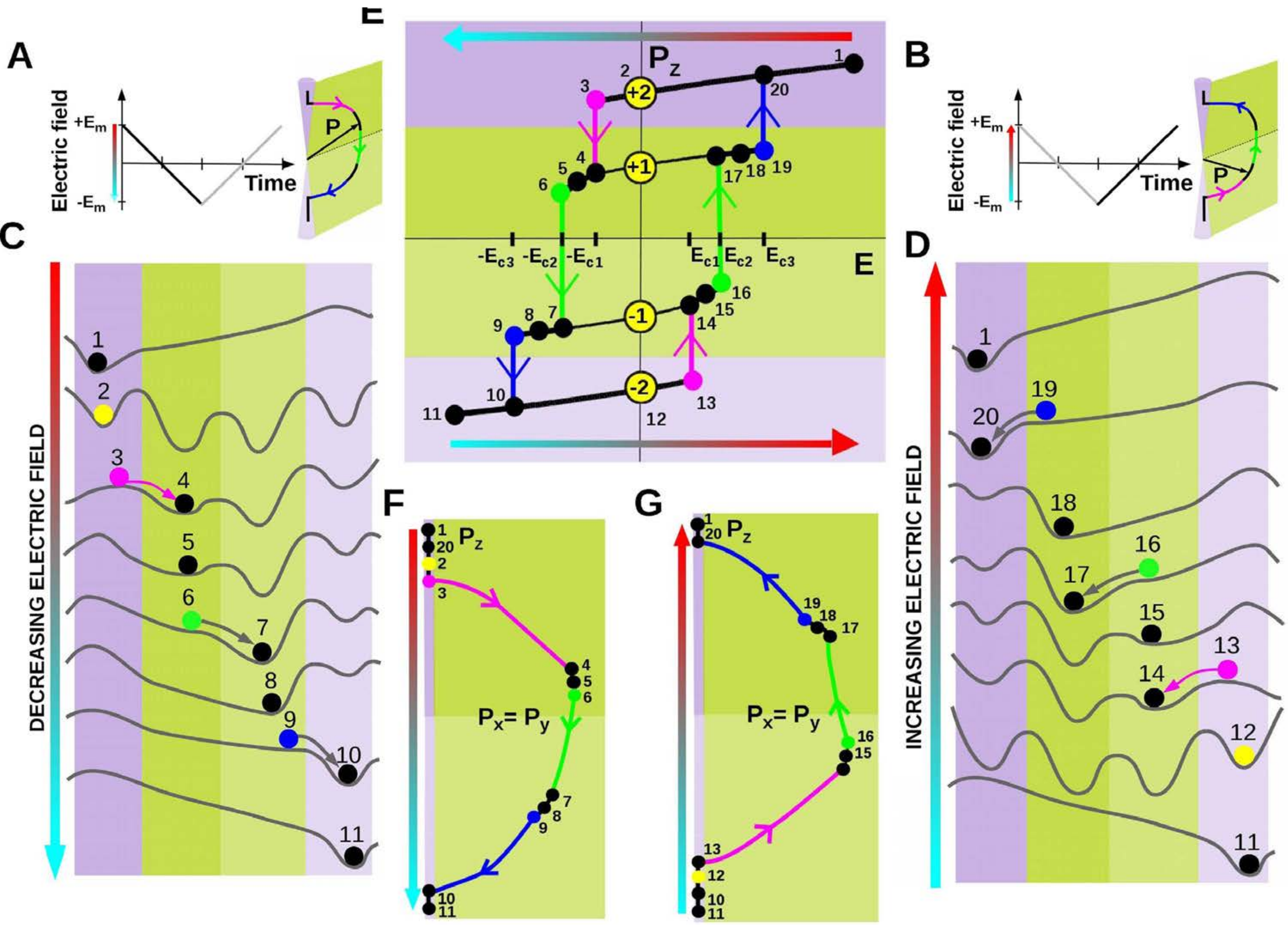
A
B
C
D
E
F
G
Electric field
+E_m
-E_m
Time
P
P_z
+2
+1
-1
-2
-E_c3
-E_c2
-E_c1
E_c1
E_c2
E_c3
DECREASING ELECTRIC FIELD
INCREASING ELECTRIC FIELD
P_x= P_y

Uniform swith phase diagram, PbTiO3

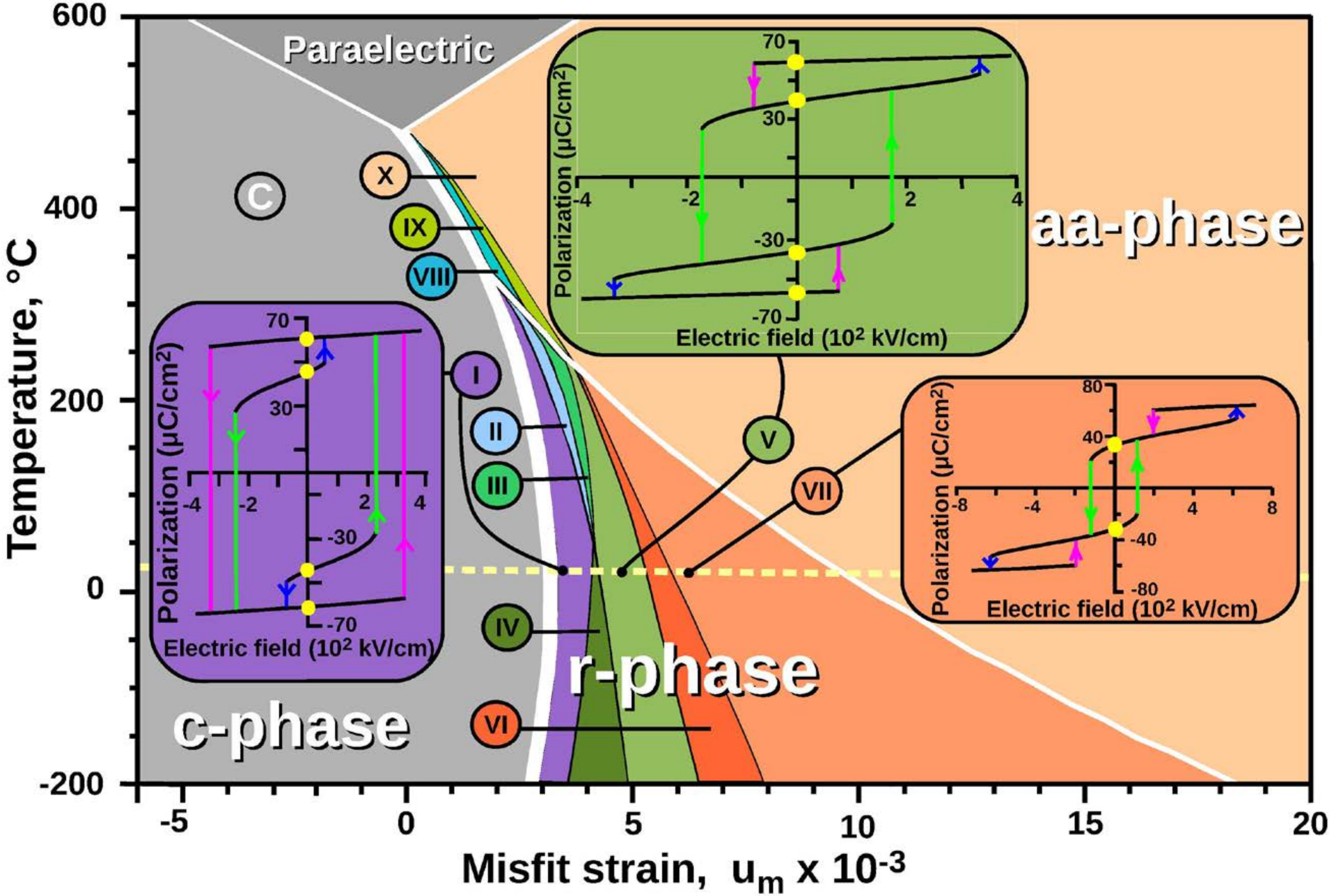

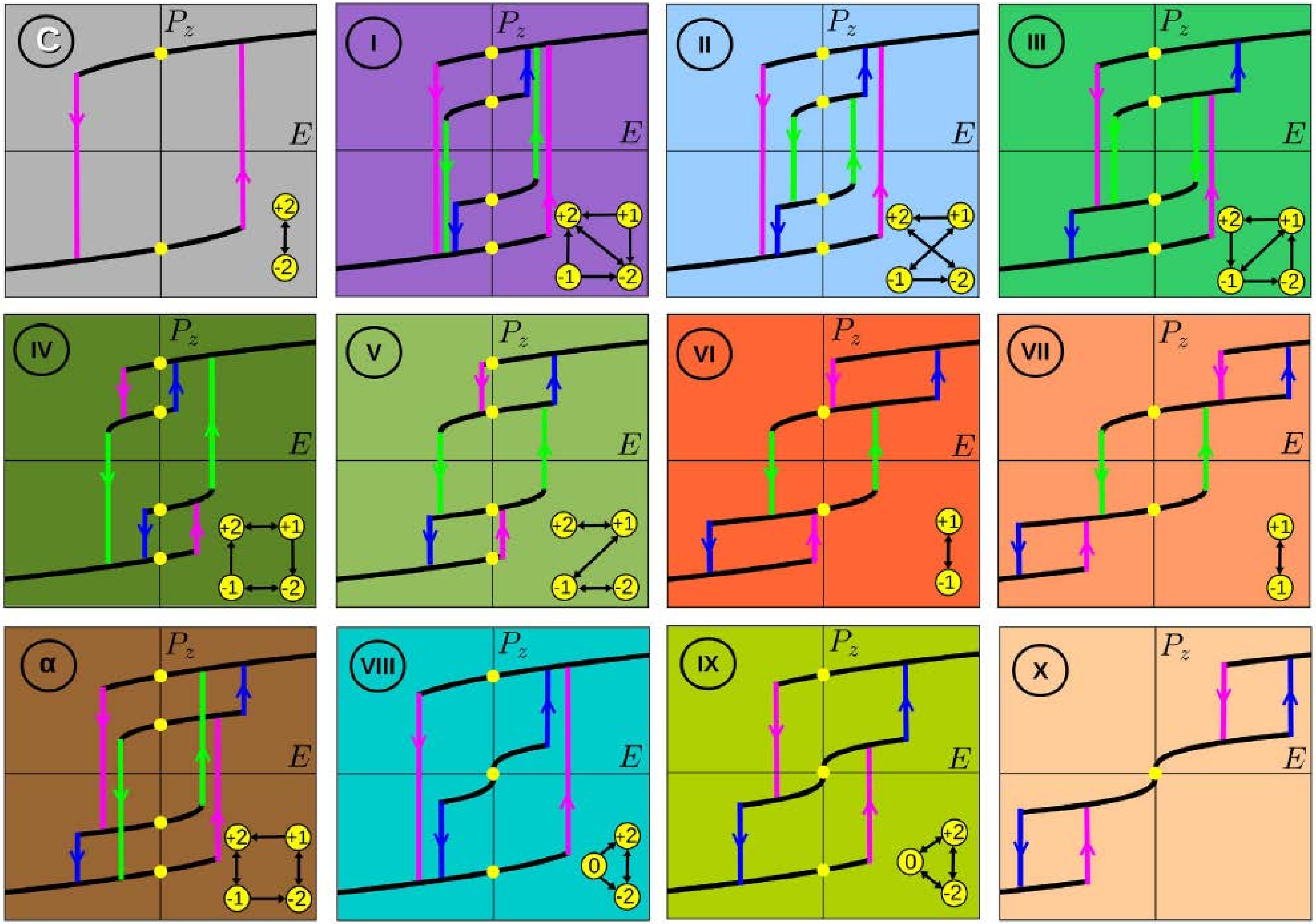

C
I
II
III
IV
V
VI
VII
α
VIII
IX
X
P_z
E
+2
+1
-1
-2
0

TOPLOGICAL ACCESS MEMORY (TAM)

Topology is strain- and temperature - tuneable

- 3 Level: *"yes", "may be" "no"*

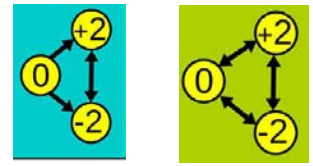

- 4 Level: *"yes", "either yes or no "*
"neither yes nor no", no"

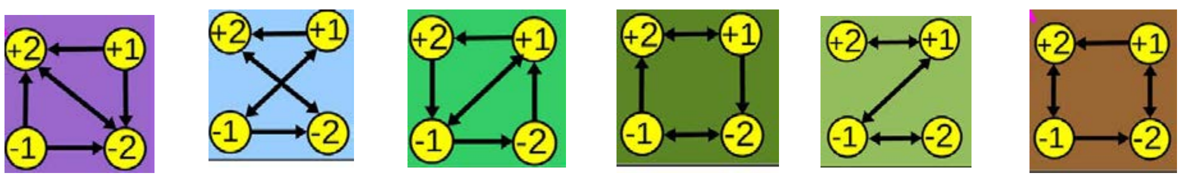

Towards non-deterministic
and neuromorphic computing

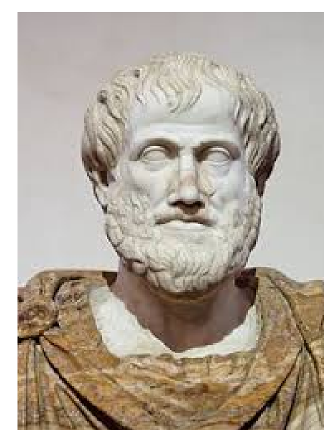

Switching of Topological Structures in Ferroelectric nano-dots:

Domains, Vortices and Skyrmions

Electrostatics is important : Q=divP=0

…

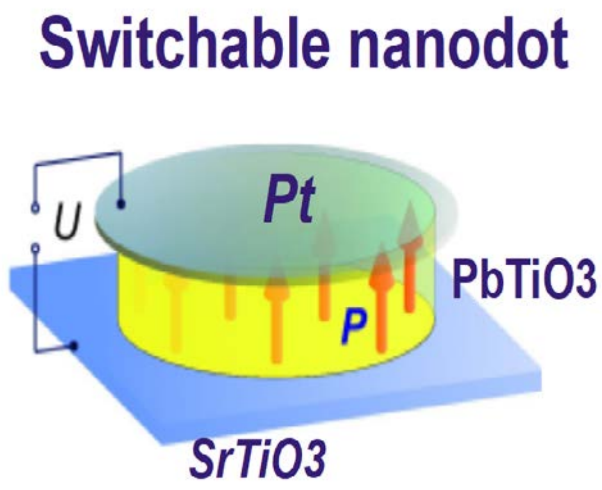

Confinement geometry

Finite size samples with:

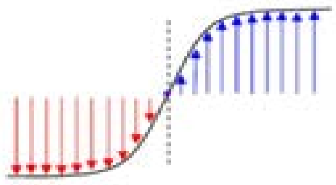

1D - easy axis polarization

=> domains

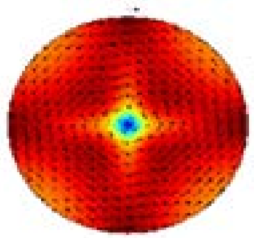

2D - easy-plane polarization

=> vortices

3D - sphere homotopy group S2

=> skyrmions

On the quantitative level:

Anatomy of GL functional

Strain-induced anisoropy *(uniaxial, easy axis…)*

Absolute value of P is involved

Interaction with E

$$\mathcal{F} = a_1^* \left(P_1^2 + P_2^2\right) + a_3^* P_3^2 + \frac{B_1}{4}\mathbf{P}^4 + \frac{B_2}{4}\sum_{x,y,z} P_i^4 - \frac{\varkappa}{4\pi}\mathbf{E}\mathbf{P}$$

$$+\frac{\xi_1^2}{2}\mathrm{div}^2\mathbf{P} + \frac{\xi_2^2}{2}\mathrm{rot}^2\mathbf{P} + \frac{\xi_3^2}{2}\sum_{x,y,z}\left(\partial_i P_i\right)^2$$

Gradient of P induces the depolarization charge ρ=divP

Crystalline anisoropy *(assumed to be weak…)*

1D

NaNO2, 16x3nm

Multidomain switching in the ferroelectric nanodots

Pierre-William Martelli, Séraphin M. Mefire and Igor A. Luk'yanchuk

EPL, **111** (2015) 50001

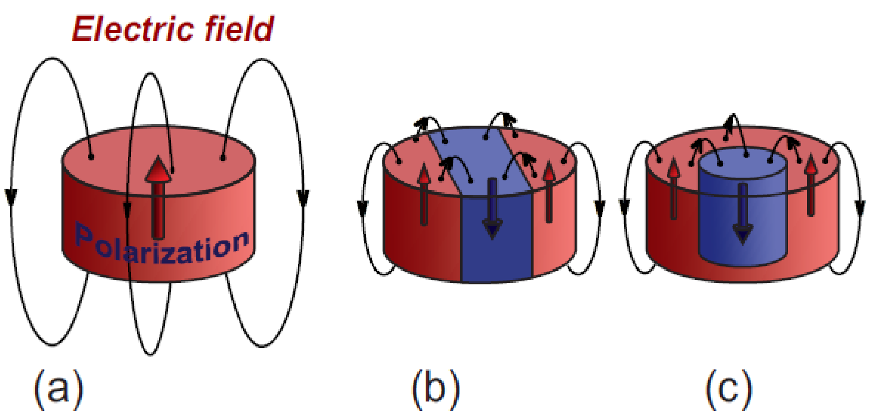

Mathematics…phase field method

$$\left(t + \frac{P^2}{P_0^2} - \xi_{0x}^2\partial_x^2 + \xi_{0y}^2\partial_y^2 - \xi_{0||}^2\partial_z^2\right)P = -\frac{\kappa_{||}}{4\pi}\partial_z\varphi$$
$$\left(\varepsilon_x\partial_x^2 + \varepsilon_y\partial_y^2 + \varepsilon_{i||}\partial_z^2\right)\varphi = 4\pi\partial_z P$$

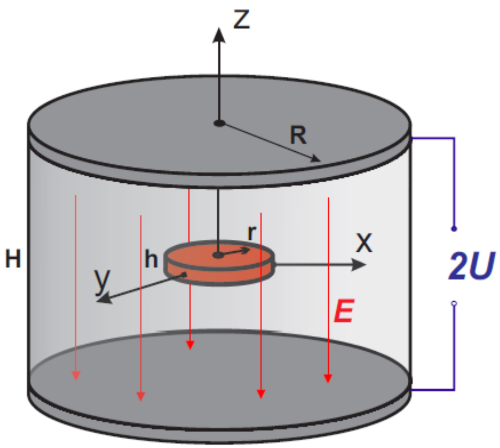

Boundary conditions at S_{fp}
at the upper/lower surfaces:

$$\varepsilon_{||}\partial_z\varphi + 4\pi P = \varepsilon_p\partial_z\varphi_p, \quad \varphi_p = \varphi$$
$$\partial_z P = 0$$

at the lateral surface, $\mathbf{n} = (n_x, n_y, 0)$

$$\varepsilon_\perp\nabla_\perp\varphi = \varepsilon_p\nabla_\perp\varphi_p, \quad \varphi_p = \varphi$$

$$(\mathbf{n}\nabla)P = 0$$

Phase diagram, … different metastable states

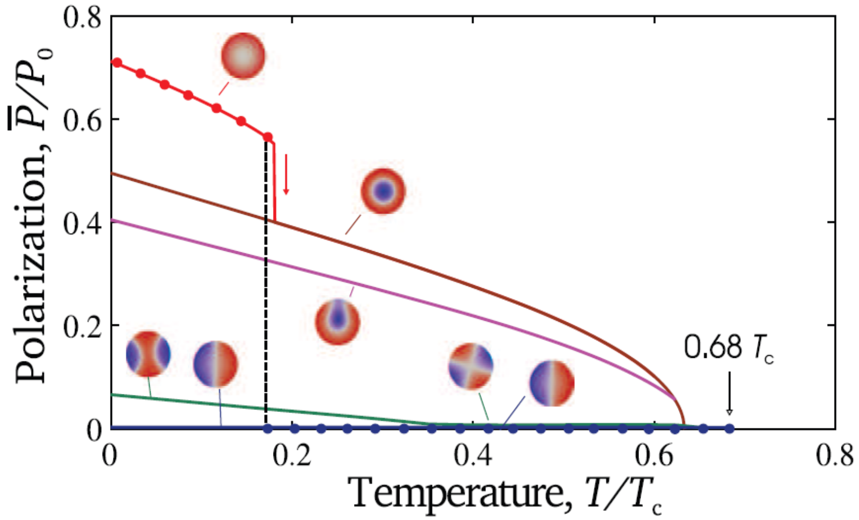

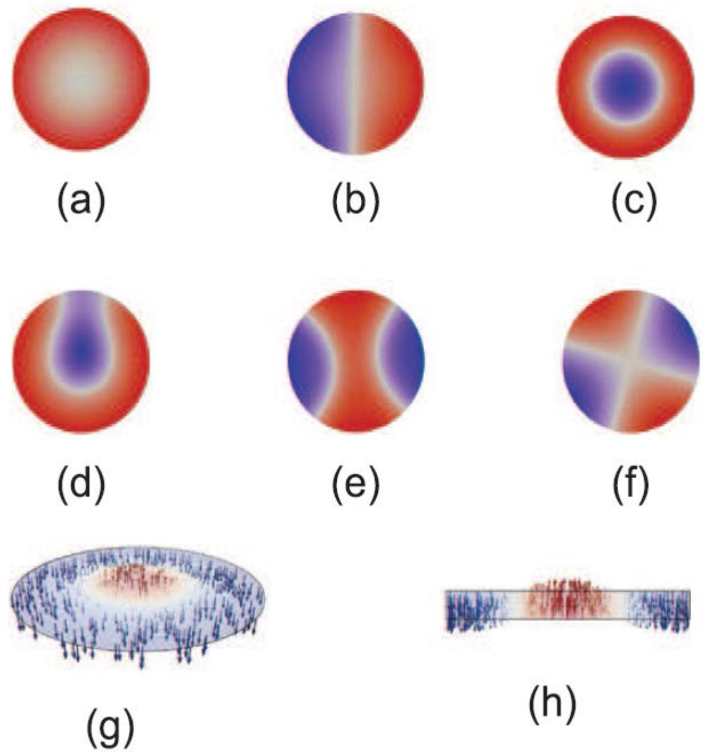

4-bit switching ….

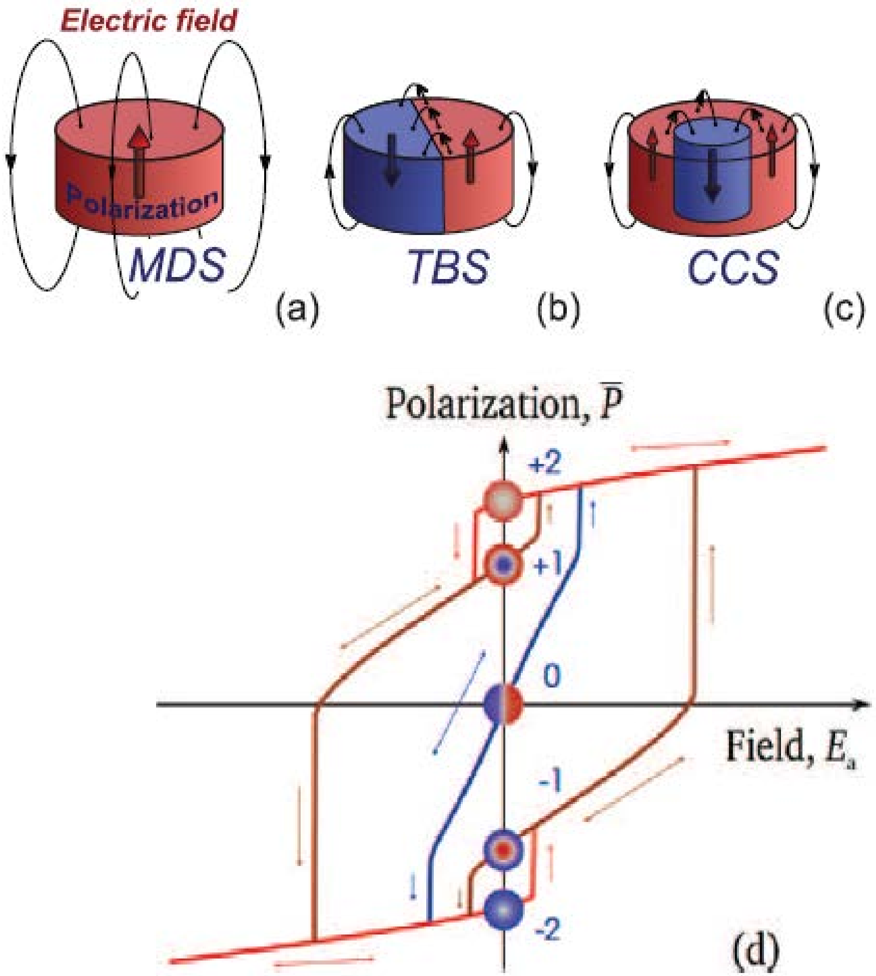

More details…

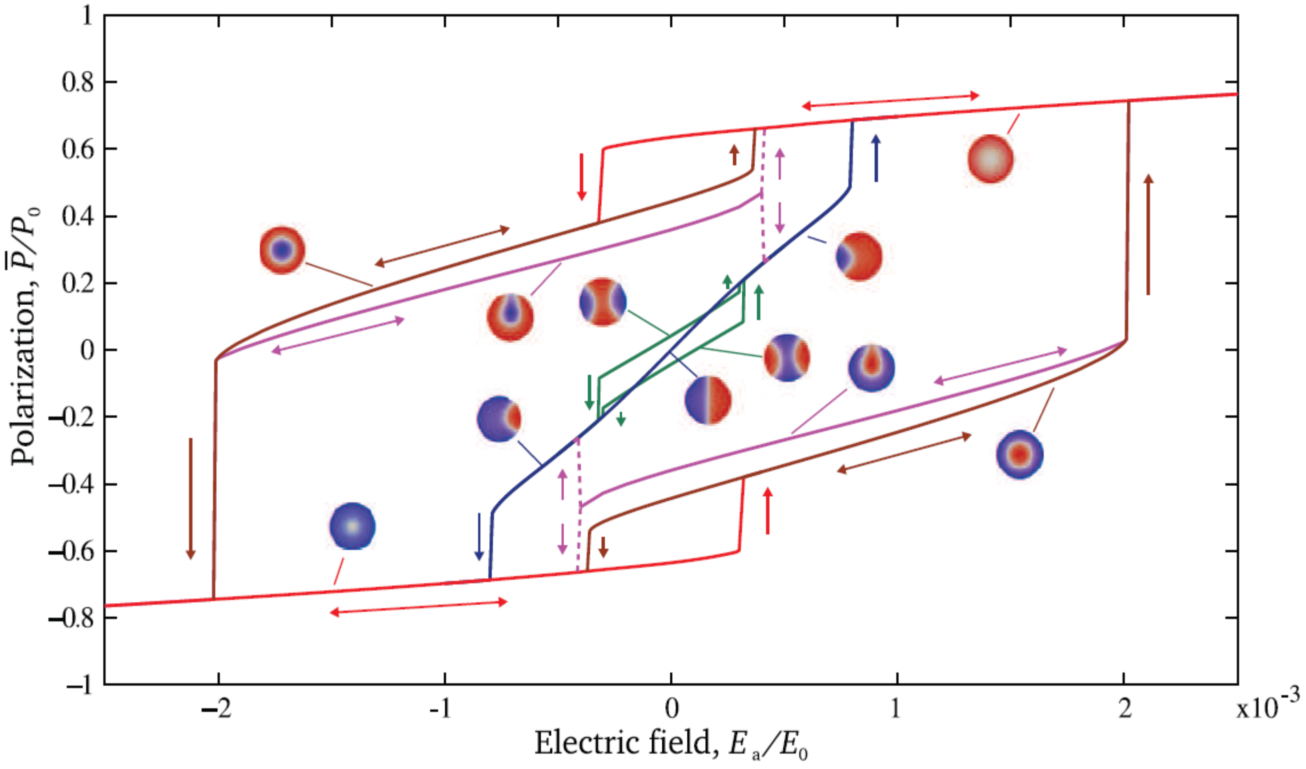

dx.doi.org/10.1021/nl503070f | *Nano Lett.* 2014, 14, 6931−6935

NANO LETTERS

Letter

pubs.acs.org/NanoLett

High-Symmetry Polarization Domains in Low-Symmetry Ferroelectrics

I. Lukyanchuk,[*,†,‡] P. Sharma,[§] T. Nakajima,[∥] S. Okamura,[∥] J. F. Scott,[⊥] and A. Gruverman[*,§]

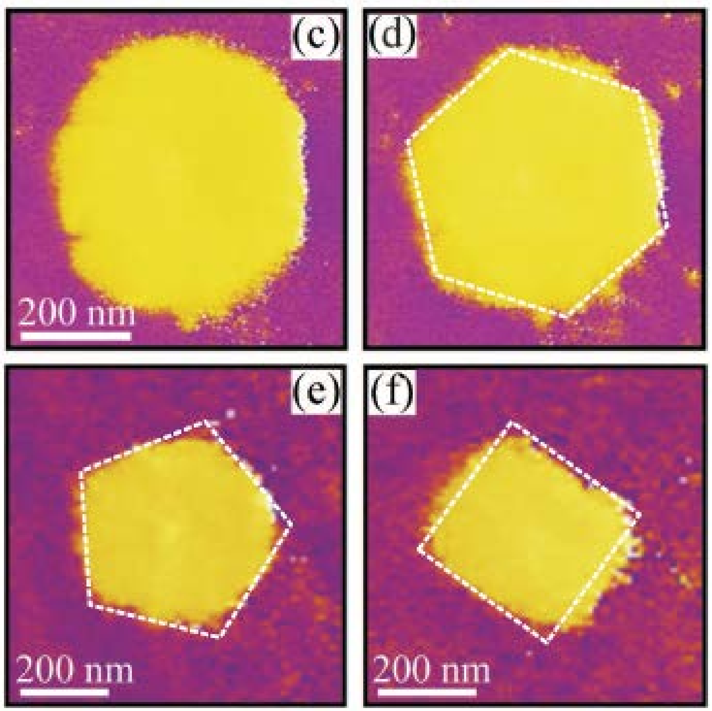

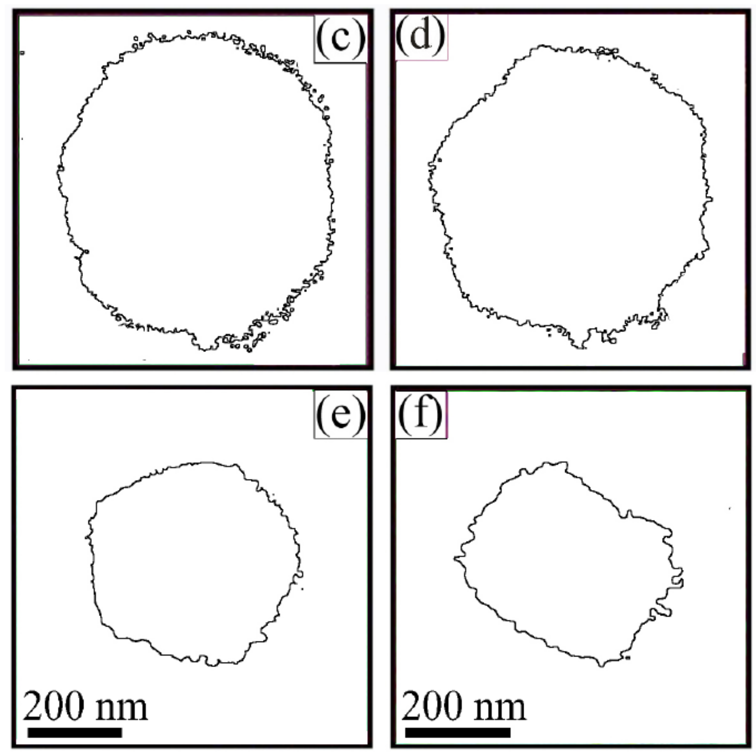

PFM immage in **PVDF-TrFE** 50nm films

Study of the real capacitor

Gustav Robert Kirchhoff
(1824-1887)

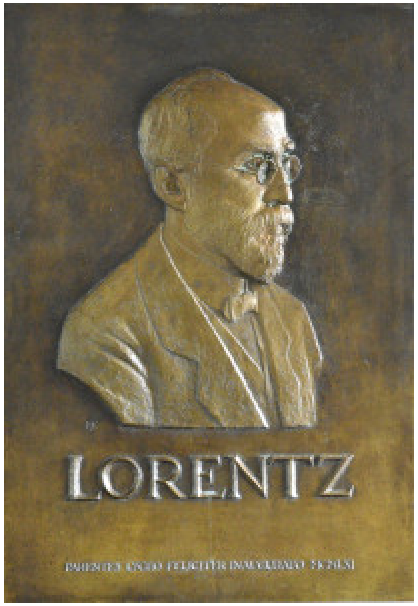

Kirchhoff 1877 (*Monatsb. Deutch. Acad*.)
Lorentz 1879 (Wied. Ann.)

Energy of the real capacitor

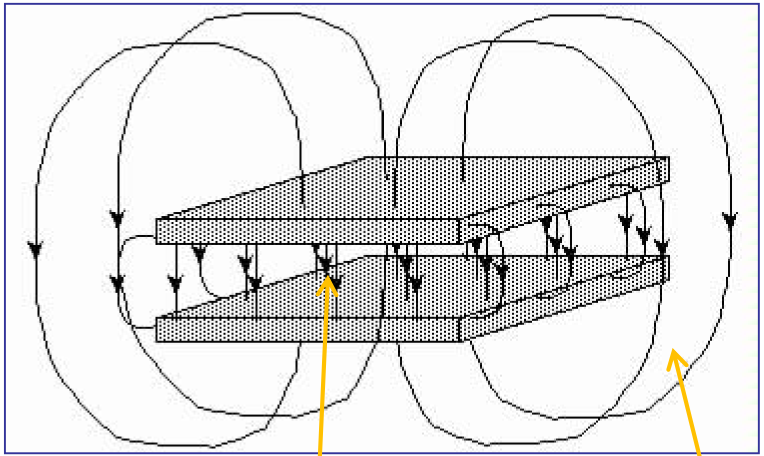

Bulk contribution

Fringing field

$$W = \frac{Q^2}{2C} = \frac{1}{2\varepsilon_0\varepsilon_{\parallel}} h^2 (2P)^2 S - (2\pi r)\, h^2 (2P)^2 \ln \frac{8r}{e^{1/2} h}$$

- Negative !
- Nonlocal !

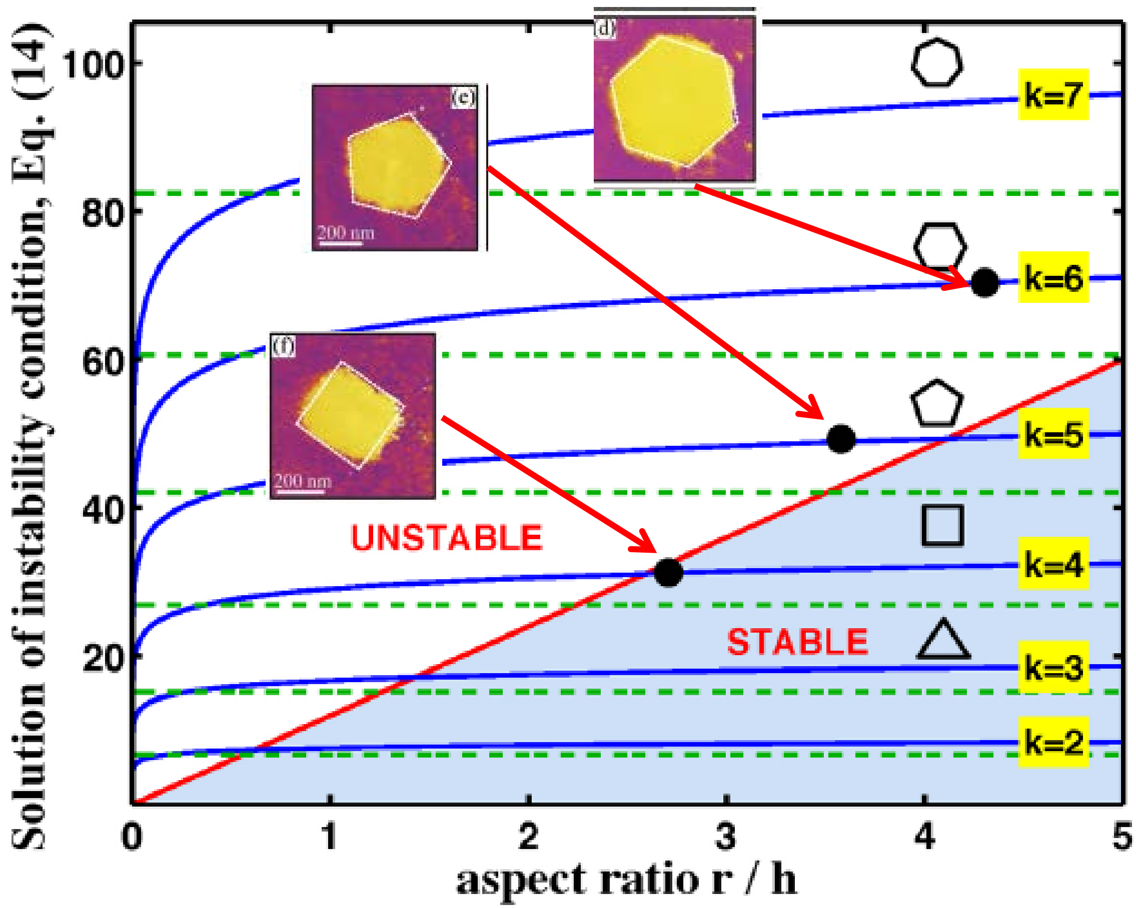

Solution of instability condition, Eq. (14)
100
80
60
40
20
0
1
2
3
4
5
aspect ratio r / h
k=7
k=6
k=5
k=4
k=3
k=2
UNSTABLE
STABLE
(c)
(d)
(f)
200 nm
200 nm

IOP PUBLISHING NANOTECHNOLOGY
Nanotechnology 24 (2013) 015706 (6pp) doi:10.1088/0957-4484/24/1/015706

Effect of disorder potential on domain switching behavior in polymer ferroelectric films

Pankaj Sharma[1], Takashi Nakajima[2], Soichiro Okamura[2] and Alexei Gruverman[1]

Another condition (opposite field)

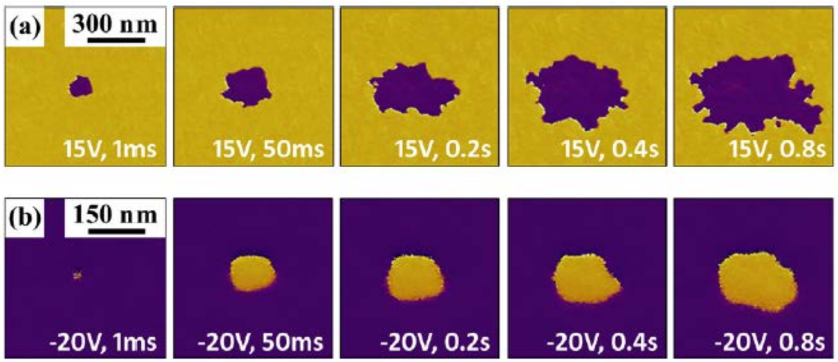

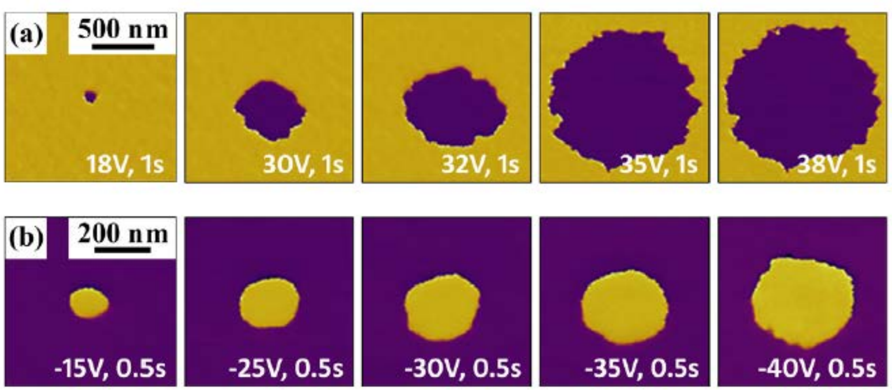

STABILITY OF VORTEX PHASES IN FERROELECTRIC EASY-PLANE NANO-CYLINDERS

L. LAHOCHE [a]; I. LUK'YANCHUK [b]; G. PASCOLI [c]

Online Publication Date: 01 January 2008

2D

Most stable

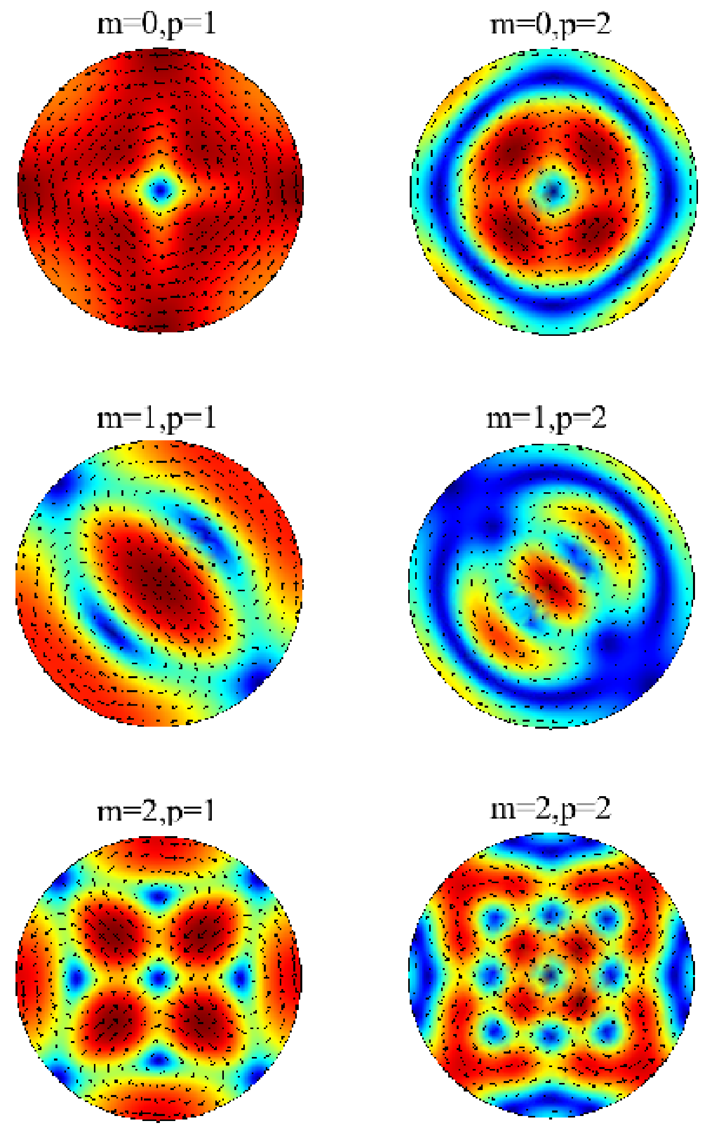

Mathematics…

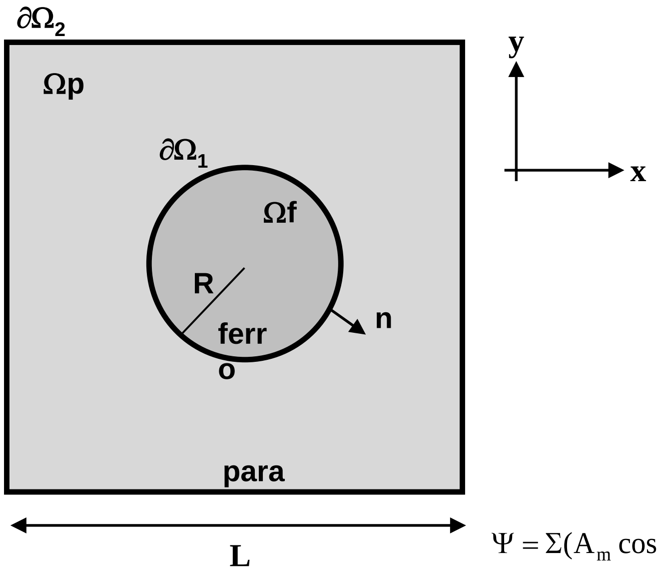

- Numerical
- Analytic

$$\nabla^2\varphi^{(f)} = 4\pi\nabla P$$

$$4\pi\varepsilon_{//}^{-1}[(t + P^2)P - \xi_0^2\nabla^2 P] = -\nabla\varphi^{(f)}$$

$$\Psi = \Sigma(A_m \cos m\theta + B_m \sin m\theta) J_m(k_1\rho)$$

, **(15)**

$$\Phi = \Sigma[C_m \frac{J_m(k_2\rho)}{J_m(k_2 R)} + \varepsilon_{//}\frac{E_m}{K_2^2}(\frac{\rho}{R})^m]\cos m\theta + [D_m \frac{J_m(k_2\rho)}{J_m(k_2 R)} + \varepsilon_{//}\frac{E_m}{K_2^2}(\frac{\rho}{R})^m]\sin m\theta$$

, **(16)**

$$\varphi^{(f)} = \Sigma[C_m \frac{J_m(k_2\rho)}{J_m(k_2 R)} + \varepsilon_{//}E_m \frac{K_1^2}{K_2^2}(\frac{\rho}{R})^m]\cos m\theta + [D_m \frac{J_m(k_2\rho)}{J_m(k_2 R)} + \varepsilon_{//}F_m \frac{K_1^2}{K_2^2}(\frac{\rho}{R})^m]\sin m\theta$$

, **(17)**

$$\varphi^{(p)} = \Sigma(G_m \cos m\theta + H_m \sin m\theta)(\frac{R}{\rho})^m$$

.

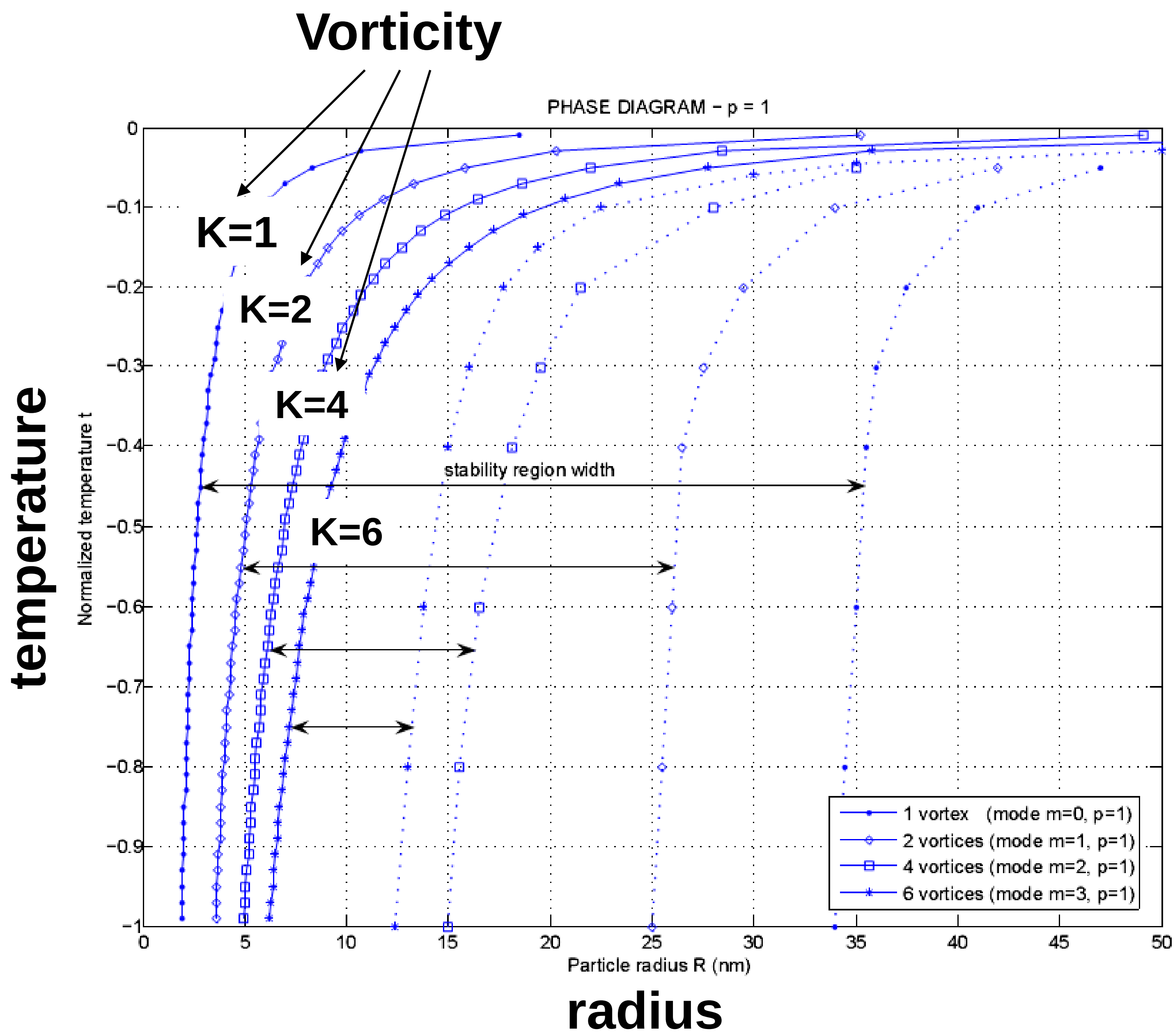
Vorticity
PHASE DIAGRAM - p = 1
K=1
K=2
K=4
K=6
stability region width
temperature
Normalized temperature t
radius
Particle radius R (nm)
0
-0.1
-0.2
-0.3
-0.4
-0.5
-0.6
-0.7
-0.8
-0.9
-1
0
5
10
15
20
25
30
35
40
45
50
1 vortex (mode m=0, p=1)
2 vortices (mode m=1, p=1)
4 vortices (mode m=2, p=1)
6 vortices (mode m=3, p=1)

3D

Chiral skyrmions

Superlattices and Microstructures 49 (2011) 314–317

Contents lists available at ScienceDirect

Superlattices and Microstructures

journal homepage: www.elsevier.com/locate/superlattices

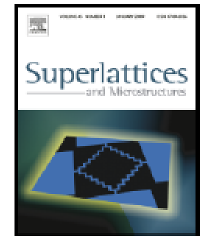

ELSEVIER

Field-induced vortices in weakly anisotropic ferroelectrics

A. Sené[a,*], L. Baudry[b], I. Luk'yanchuk[a], L. Lahoche[c], Y. El Amraoui[d]

PHYSICAL REVIEW B **90**, 024102 (2014)

Polarization vortex domains induced by switching electric field in ferroelectric films with circular electrodes

Laurent Baudry,[1,*] Anaïs Sené,[2] Igor A. Luk'yanchuk,[3] Laurent Lahoche,[2] and James F. Scott[4]

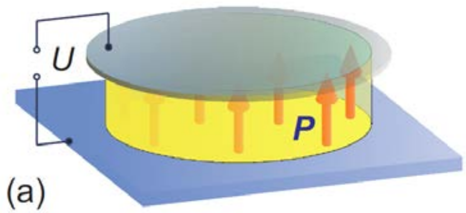

Polarization Switching in Ferrelectric Nanodot

Uniform switching | **Domain nucleation** | **Polarization rotation**

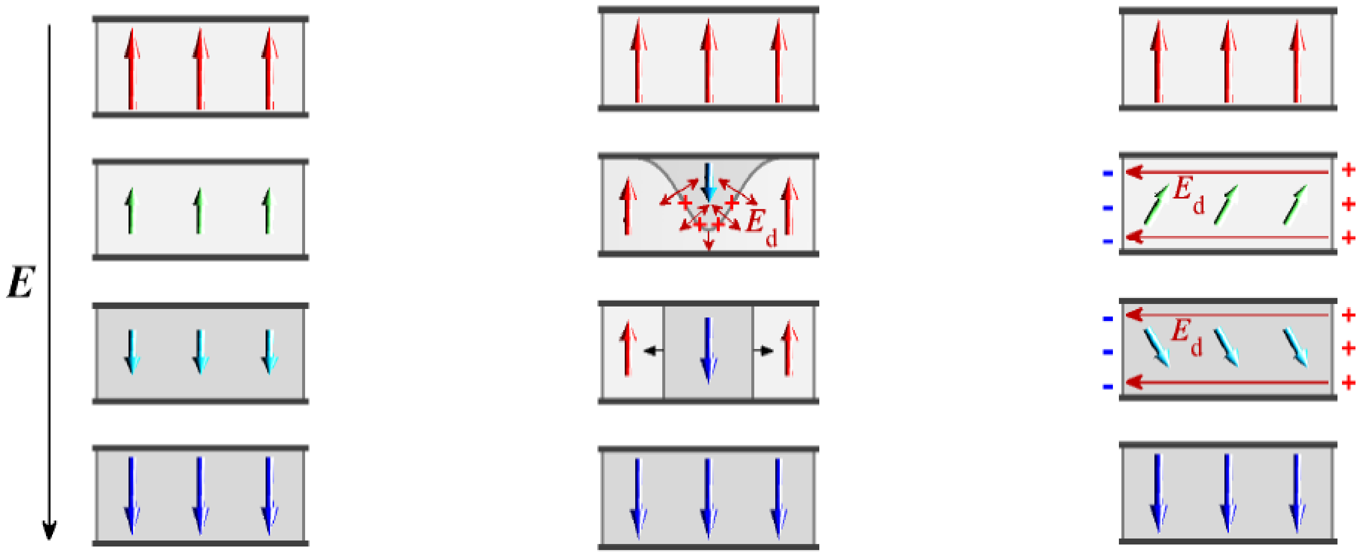

Very high coercive field (*Landauer Paradox*), because of the *depolarization field*

Torsion instability

No depolarization charge,
div P = 0 !!!

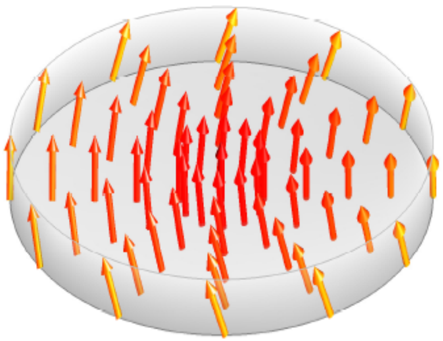

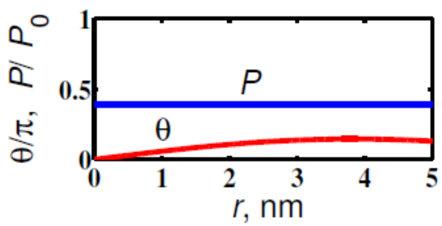

Low coercive field !

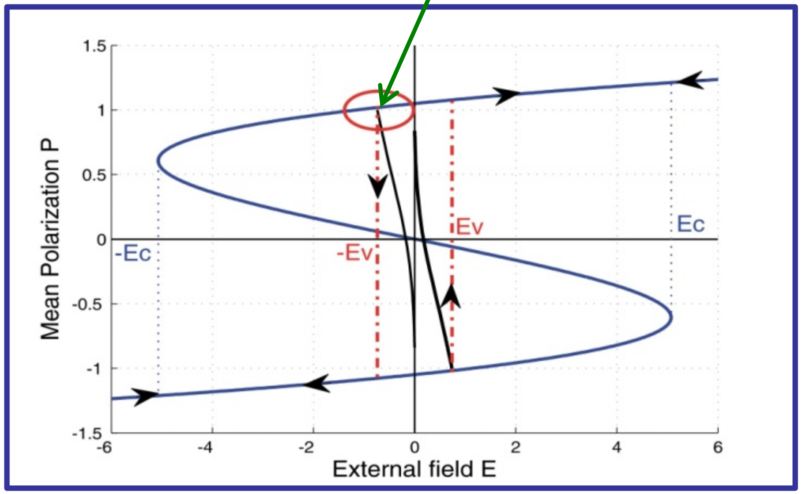

Linear stability analysis

$$\tilde{\mathcal{F}} = \frac{1}{2}\left(t + \mathcal{L}\left(\theta, \theta', r\right)\right) P^2 + \frac{P_0^{-2}}{4} P^4 + \frac{\xi_0^2}{2} P'^2 + \frac{\xi_0^2}{2}\left(P \sin\theta\right)^{2\prime} - eP\cos\theta$$

Further evolution:
Skyrmion formation

Chiral (Bloch)
Structure with *divP=0*

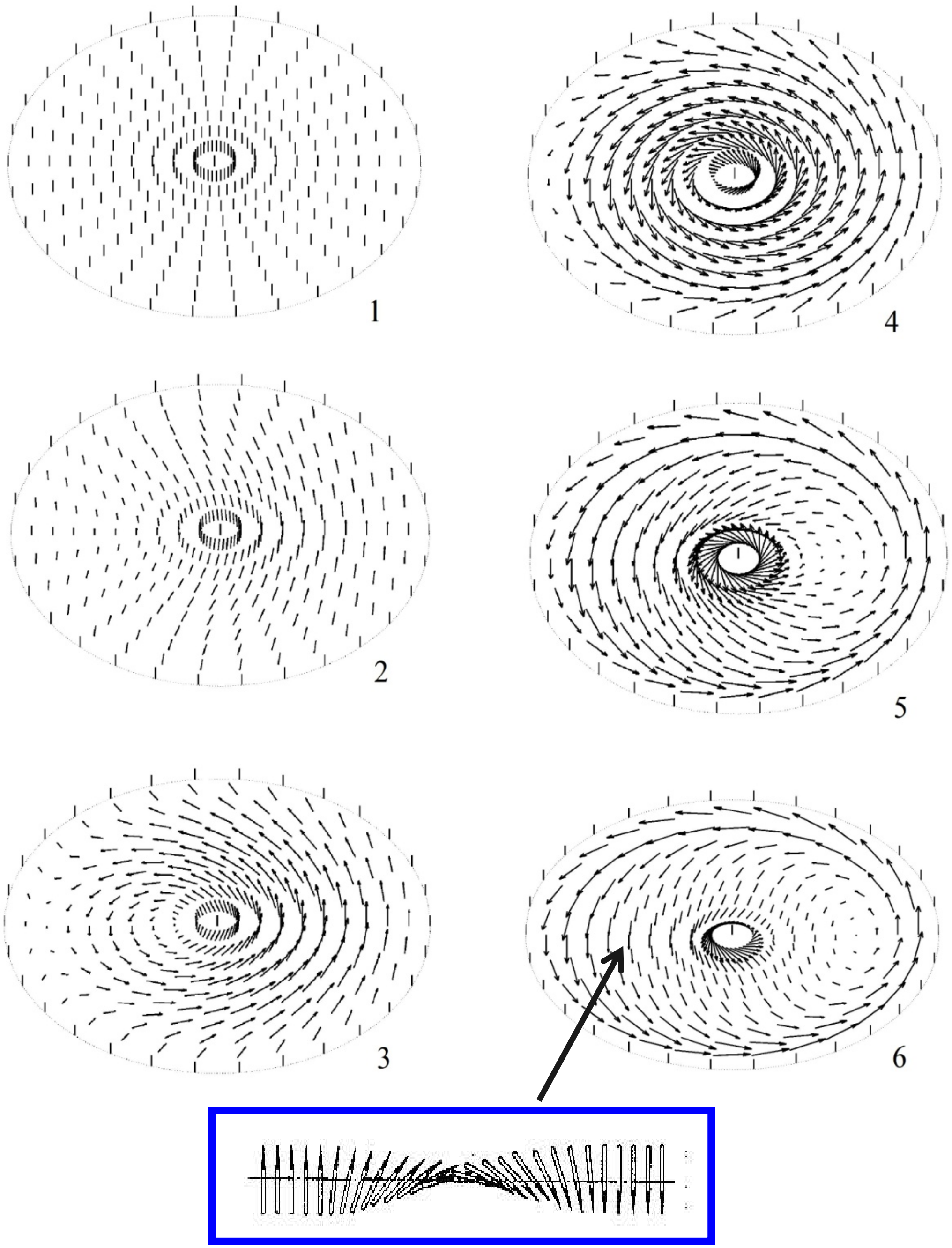

Nonlinear equations with *P*-θ coupling

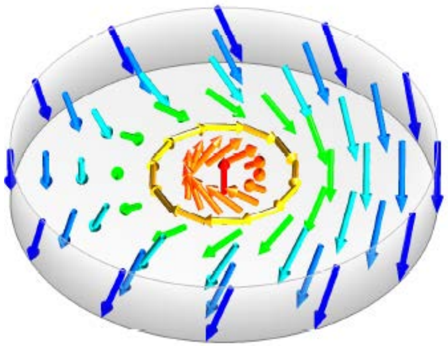

$$\nabla_r^2\theta = \left[\alpha + \frac{1}{2r^2}\right]\sin 2\theta + eP\sin\theta,$$

$$\xi_2^2\nabla_r^2 P = \left[t + \mathcal{L}(\theta,\theta',r)\right]P + bP^3 - e$$

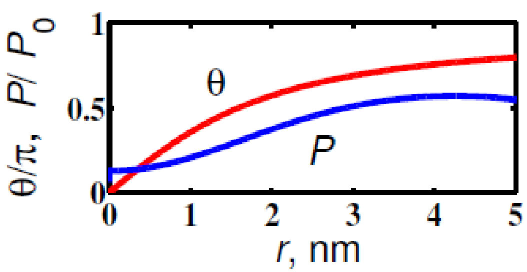

$$\mathcal{L}(\theta,\theta',r) = a\sin^2\theta + \xi_0^2\theta'^2 + \frac{\xi_0^2}{r^2}\sin^2\theta$$

CONCLUSION …

Nanopillars

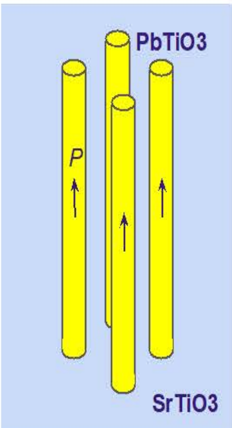

1D, easy axis polarization

Domain Walls

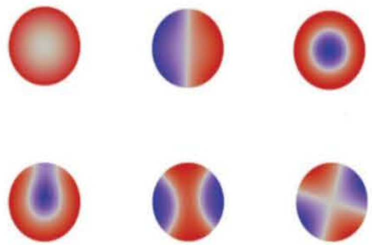

2D, easy plane polarization

in-plane Vortices

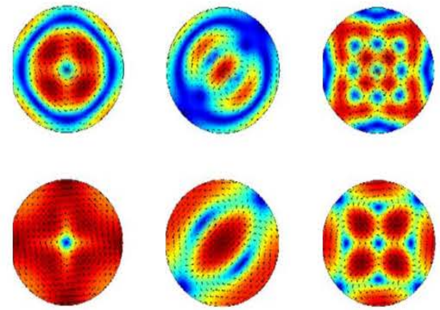

3D, quasi-isotropic

Skyrmions

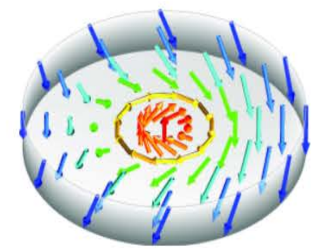

Switchable nanodot

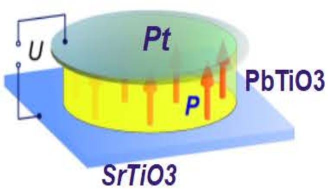

5-level logic

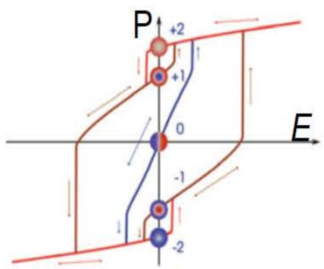

3-level logic

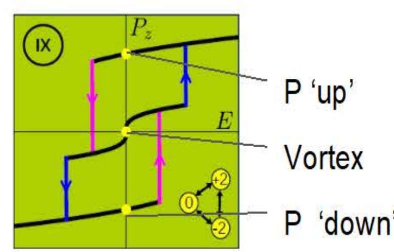

4-level logic

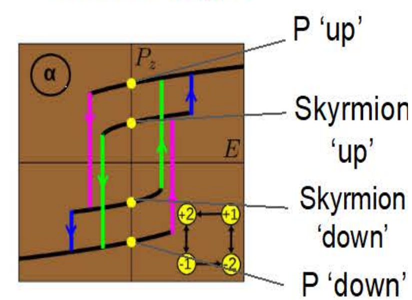


“Topological Structures in Ferroic Materials”
in *International Institute of Physics, IIP*
Natal Brazil, June 2018
TOPO 2018
ORGANIZERS:
José Antonio Eiras, *University of Sao Carlos, Brazil*,
Igor Lukyanchuk, *University of Picardie, France*,
Jan Seidel *University of New South Wales, Australia*,


INTERNATIONAL INSTITUTE OF PHYSICS
www.iip.ufrn.br

INTERNATIONAL ADVISORY COMMITTEE

8-10 International Workshops are selected per year

Alfredo Ozório de Almeida
CBPF/ Brazil

Alvaro Ferraz
DFTE-UFRN / Brazil

Amir Ordacgi Caldeira
Condensed Matter Physics Department, UNICAMP / Brazil

Beatriz Leonor Silveira Barbuy
IAG, University of São Paulo/ Brazil

Claudionor Gomes Bezerra
DFTE-UFRN/ Brazil

David Gross
Kavli Instutute of Theoretical Physics / USA

David R. Nelson
Department of Physics, Harvard University / USA

Dionys Baeriswyl
Physics Department, University of Fribourg/ Switzerland

Eduardo Cantera Marino
Institute of Physics, Federal University of Rio de Janeiro/ Brazil

Gerard t'Hooft
Department of Physics, Utrecht University / Holland

Giuseppe Mussardo
SISSA, Trieste / Italy

Itamar Procaccia
Weizmann Institute of Science/ Israel

2016 - IAC MEETING

José Renan de Medeiros
DFTE-UFRN/ Brazil

Konstantin Efetov
Institute of Theoretical Physics, Ruhr-Universität Bochum/ Germany

Michael Berry
Physics Department, University of Bristol/ England

Mitchell J. Feigenbaum
Laboratory of Mathematical Physics, Rockefeller University/USA

Mucio Continentino
CBPF / Brazil

Nathan Berkovits
SAIFR-UNESP/ Brazil

Sandra Denise Prado
Physics Institute - UFRGS/ Brazil

Silvio Salinas
Physics Institute, University of São Paulo/ Brazil

Simon White
Max-Planck Institute for Astrophysics/ Germany

Facilites:

- 2 SEMINAR ROOMS
- 2 DISCUSSION ROOMS
- 1 LARGE LECTURE ROOM
- 36 OFFICES FOR RESEARCHERS (SINGLE, DOUBLE AND TRIPLE)
- RESTAURANT FACILITIES
- ADMINISTRATION OFFICERS

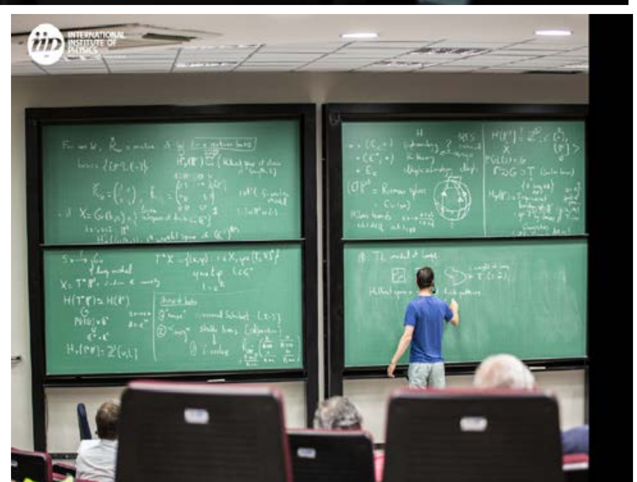

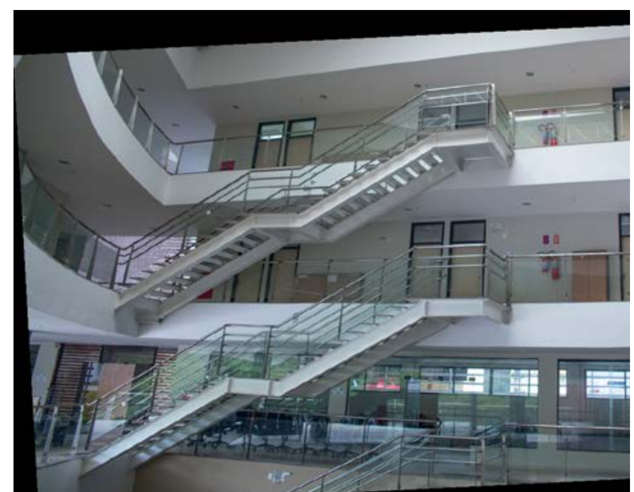

NATAL

- Population ~ 1mln
- 24-27° C in June
- Closest point to Europe
- 600 km South from Equator
- Major tourist destination in Brazi
- Gateway to stunning beaches

360+ hotels

Lisbon – Natal (TAP-Portugal) 7h

Miami – Brasilia - Natal (AAA +) 13h

Sao Paulo – Natal, 8 flights /day 3.5h





Sun, sea, sand – and SCIENCE
www.topo2018.ferroix.net
SKOL
h&h